Quaternary International xxx (xxxx) xxx

Contents lists available at ScienceDirect

Quaternary International

journal homepage: www.elsevier.com/locate/quaint

# Environmental changes recorded in the sequence of lake-peat bogs in the Eemian Interglacial and Vistulian on the basis of multi-proxy data

Joanna Mirosław-Grabowska [a,*], Ryszard Krzysztof Borówka [b], Magdalena Radzikowska [a], Joanna Sławińska [b], Anna Hrynowiecka [c], Artur Sobczyk [d], Renata Stachowicz-Rybka [e], Krzysztof Stefaniak [f]

[a] Institute of Geological Sciences, Polish Academy of Sciences, INGPAN, Twarda St. 51/55, PL-00818, Warsaw, Poland
[b] Institute of Marine and Environmental Sciences, University of Szczecin, Mickiewicza St. 18, PL-70383, Szczecin, Poland
[c] Polish Geological Institute–National Research Institute, Marine Geology Branch, 5 Kościerska Str., PL 80-328, Gdańsk, Poland
[d] Department of Structural Geology and Geological Mapping, Institute of Geological Sciences, University of Wroclaw, M. Borna 9, 50-204, Wrocław, Poland
[e] W. Szafer Institute of Botany, Polish Academy of Sciences, Lubicz St. 46, PL-31512, Krakow, Poland
[f] Department of Palaeozoology, Institute of Environmental Biology, University of Wroclaw, Sienkiewicza St. 21, PL-50335, Wrocław, Poland

ARTICLE INFO

*Keywords:*
Lake cycles
Eemian-Vistulian
Stable isotopes
Geochemistry
NW Poland

ABSTRACT

We present the results of geochemical investigations, including stable isotope, of the Eemian (MIS 5e) and Vistulian (Weichselian, MIS 5a–d, MIS 3–4) sediments of the palaeolake horizons from Gorzów Wielkopolski site (NW Poland). Our analyzes comprised two profiles from different parts of lake basin, each approximately 11-m long. The deposits represent two cycles of lake accumulation (two limnic layers), each ended by peat deposition, separated by mineral fluvial deposits. The lower and upper limnic layers, despite several similar geochemical features, are records of two separate phases of the lake's functioning. The palynological data suggest that the mineral deposits separating them are not continuous succession, but contain a stratigraphic hiatus. We characterized six geochemical zones (GZ), which correspond well with lithological features of deposits and climatic changes, and reflect the changing environmental conditions (redox conditions, variability and intensity of denudation, biological productivity, and fertility of the environment). In the first phase of lake's development, some influence of the surface material supply is visible, indicated by the increased content of lithophilous elements, (e.g. potassium), as well as closely correlated with them copper and zinc. Slow accumulation of carbonates dominated the limnic layers due to their abundant supply from the catchment area. The greatest variations of isotopic values of carbonates occur in the bottom and at the top of the stratigraphic profile and are related to the changing environmental conditions in the lake's basin (water level and temperature variations). The differences in carbon and nitrogen isotope values suggest different sources of organic matter accumulated in the studied basin and varying trophy of the environment. The higher mercury content is related to the course of climate change and is the highest in cold periods. We identified five main phases of evolution of the palaeolake at Gorzów Wielkopolski site. The lake accumulation began during the final phase of the Wartanian (Late Saalian) Glaciation (MIS 6). Initially the palaeolake harmonically developed and reached its maximum depth (Early and Middle Eemian, MIS 5e). Next the palaeolake became shallower and transformed into the peatbog (Late Eemian, MIS 5e). In the Early Vistulian period (or Early Weichselian, MIS 5a–d), the lake re-existed, initially as a flow-through lake. Finally in middle Vistulian (or Middle Weichselian – Pleniglacial, MIS 3–4), the palaeolake declined and mire developed.

## 1. Introduction

The Eemian and Early Vistulian (MIS 5e–d–c) lacustrine successions are common in central and eastern Poland (e.g., Bińka et al., 2006; Kupryjanowicz, 2008; Rychel et al., 2014; Hrynowiecka et al., 2018; Kupryjanowicz et al., 2018; Majecka et al., 2018; Mirosław-Grabowska et al., 2018; Wachecka-Kotkowska et al., 2018; Woronko et al., 2018; Żarski et al., 2018, Roman et al., 2021). Nevertheless up until now, only

* Corresponding author.
*E-mail address:* jmirosla@twarda.pan.pl (J. Mirosław-Grabowska).

https://doi.org/10.1016/j.quaint.2021.11.023
Received 3 July 2021; Received in revised form 23 November 2021; Accepted 27 November 2021
Available online 30 November 2021

a few Eemian-Early Vistulian sites were known in north-western Poland for example at Rzecino (Mirosław-Grabowska, 2008; Winter et al., 2008; Niska and Mirosław-Grabowska, 2015), Radówek (Urbański and Winter 2005) and Słubice (Skompski, 1980; Alexandrowicz and Alexandrowicz, 2010)(Fig. 1). The Eemian and Early Vistulian lacustrine sediments are even rarer from north Poland – Łęczyce site (Sokołowski et al., 2015 and more detailed results in preparation for publishing). The newest site of these sediments is located in Gorzów Wielkopolski site (Sobczyk et al., 2020). This succession is one of the first of this age to be analyzed as regards the isotopic and geochemical composition of the lake-peat bog deposits in western Poland. Similar studies were carried out at Jałówka site in NE Poland and containing the sediments from the late Wartanian to the Eemian optimum (Rychel et al., 2014). The succession in Gorzów Wielkopolski site is also an unique example of the Eemian sediments in Poland, due to the very high content of carbonate sediments, comparable only to the Ruszkówek site (Mirosław-Grabowska et al., 2009).

Unfortunately, some of the Eemian–Early Vistulian successions are incomplete because (1) accumulation ended by a complete decline of the lake already in the middle Eemian or (2) lake accumulation was interrupted by peat accumulation. In the second case, a thick lacustrine sequence (lake – peatbog – lake – etc.) should be regarded as one reservoir with two or more lake phases separated by swamp phases or as separate lakes filling only one lake basin. Such an example is the succession in Gorzów Wielkopolski site (NW Poland) comprising 11-m long the lake-peatbog sequence (main profile – GS3) accumulated from the Late Wartanian, entire Eemian, and the Early Vistulian (Sobczyk et al., 2020). There are two thick layers (limnic cycles?) of lacustrine deposits (gyttja and limnic chalk) divided by peat and non-organic mineral layers accumulated in different times as well as climatic conditions. The changing climate affected the environmental conditions in the reservoir, reflecting in the composition of these sediments and biological life. In these sediments the remains of Merck's rhinoceros *Stephanorhinus kirchbergensis* (Jäger, 1839) were found (Badura et al., 2017; Sobczyk et al., 2020).

This paper presents the results of mainly isotopic and geochemical studies of the Eemian (MIS 5e) and Vistulian (MIS 5a–d, MIS 3–4) deposits from Gorzów Wielkopolski site. Especially we focus on the comparison of the features of two lake layers concerning the possible climatic changes and environmental conditions. We reconstruct the evolution phases of the studied lake basin. We wonder if the lake phases were characterized by similar conditions or were absolutely different.

## 2. Regional setting

The studied palaeolake (52°43′51" N; 15°09′33" E) is located in Gorzów Wielkopolski city (Gorzów Plain, western Poland, Fig. 1). The research material of GS1 and GS3 (main) profiles was exposed during the construction of the S3 express road (Fig. 2). An 11-m-thick sediment sequence from the GS3 profile (two layers of gyttja and lacustrine chalk separated by peat and fluvial sands and silts) reflects the multi-phase development of the palaeolake. In addition almost complete skeleton of *Stephanorhinus kirchbergensis*, including a skull with 24 well-preserved teeth, discovered in the lower part of the palaeolake sediments. Apart from the rhinoceros remains, a single metacarpal bone of fallow deer (*Dama dama*) was found on the site (Badura et al., 2017; Sobczyk et al., 2020). The unique sediments have been analyzed for multi-proxy analyses e.g. geochemical, zoological, palynological, etc. (Sobczyk et al., 2020; Stefaniak et al., 2020; Alexandrowicz et al., 2021).

In the GS3 profile, Wartanian (Saalian) fluvioglacial sands and gravels occur at the bottom (Fig. 3). They are overlain by the lacustrine-

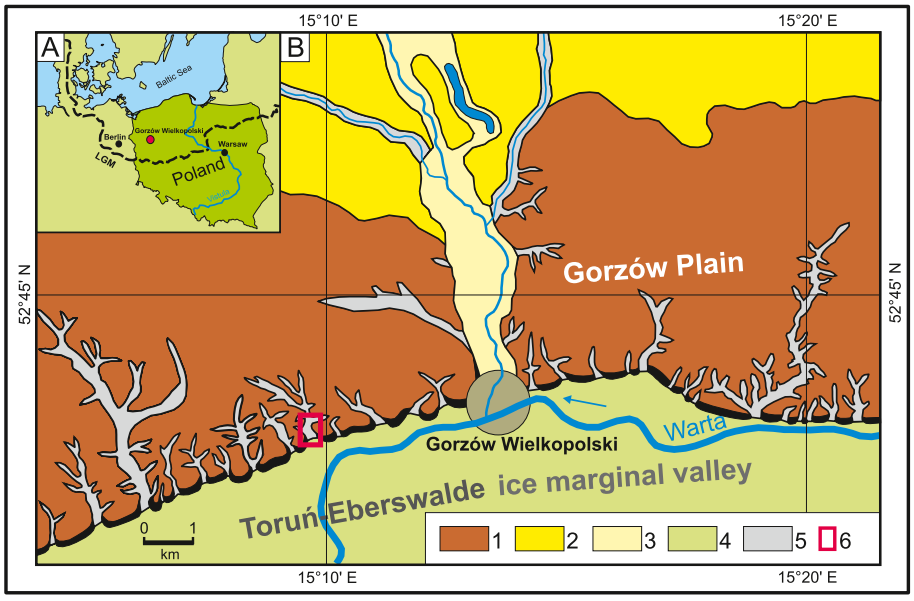


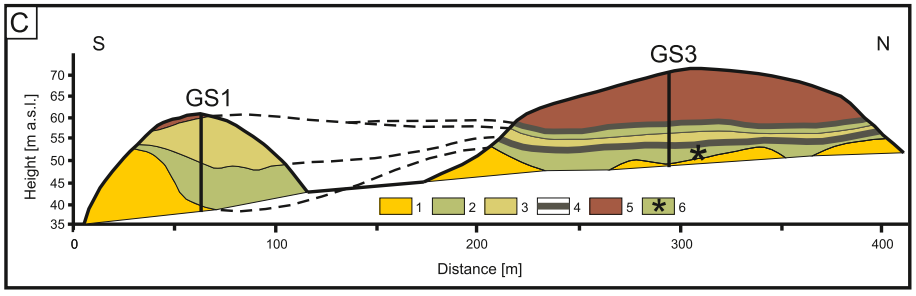


**Fig. 1.** Study area. A: Location of the studied succession in western Poland: LGM – Last Galcial Maximum limit. B: Geomorphological scheme, demonstrated location of the studied site within the relief features: 1 – morainic plateau; 2 – outwash plain; 3 – alluvial plain; 4 – ice marginal valley plain; 5 – erosional valleys; 6 – study site. C: Correlation of the two studied profiles: GS1, GS3 – studied profiles; 1 – glaciofluvial sand and gravel; 2 – calcareous gyttja; 3 – deltaic sand and lacustrine silty sand with organic matter; 4 – peat; 5 – glacial till and sandy till (glacial diamicton); 6 – location of the rhinoceros bone remains (according to Sobczyk et al., 2020).

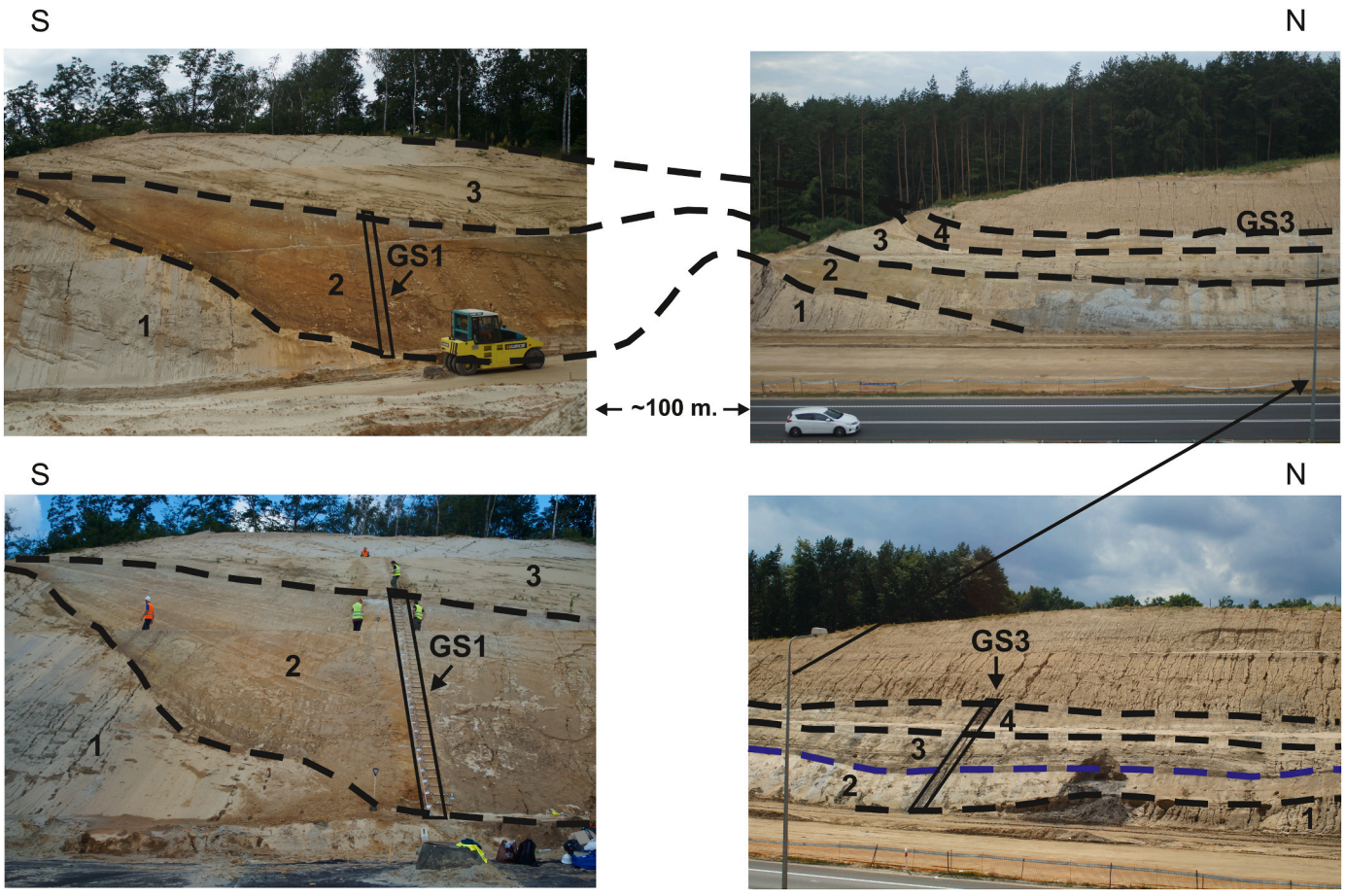


**Fig. 2.** Correlation and photos of studied profiles.
GS1, GS3 – studied profiles; 1 – glaciofluvial sand and gravel (Late Wartanian (Saalian) – MIS 6); 2 – calcareous gyttja (Eemian – MIS 5e); 3 – delta sand and lacustrine silty sand (Early Vistulian– MIS 5a–d); 4 – calcareous gyttja (Pleniglacial – MIS 3–4).

bog sediments as a yellow and greyish calcareous gyttja (lower limnic layer) with increasing $CaCO_3$ content up to 80% (thickness of ca. 3.5 m). Next dark brown peat of 0.6 m thick occurs, followed by silty sands (thickness of ca. 2 m). Then the upper limnic layer consists of light grey homogeneous limnic chalk and grey calcareous gyttja (thickness of ca. 2.2 m). The lacustrine deposits are replaced by brown peat and intercalations of silty sands and gyttja (thick of ca. 1.7 m). The uppermost of this profile consists of the Vistulian (Weichselian) fluvioglacial and glacial deposits (Badura et al., 2017).

GS1 profile is located approximately 250 m south of the GS3 profile. This profile represents a coastal part of lacustrine sediments, adjacent to palaeoslope of the lake bed formed within glaciofluvial sediments, with a maximum angle reaching 25–30° (Fig. 2). Over a distance of 50 m, the slope drops from 53 to 38 m a.s.l. The total thickness is 21.5 m, including about 11 m of lacustrine deposits. There are also mainly carbonate gyttja with the limnic chalk in the upper part. The lacustrine deposits end with fine and medium sand interbedded with silty sand (Sobczyk et al., 2020).

In this paper, we present the geochemical and isotopic results of the sediments from the GS3 profile (interval of 59.6–48.6 m a.s.l.) and from the GS1 profile (interval 51.4–40.0 m a.s.l.), representing the Late Wartanian (MIS 6), Eemian Interglacial (MIS 5e) and Vistulian (MIS 5a–d, MIS 3–4, Sobczyk et al., 2020). The correlation of the stratigraphic units of the Upper Pleistocene in Poland and Western Europ is shown in Table 1.

## 3. Material and methods

### 3.1. Geochemical analyses

Geochemical analyses of sediments from GS1 and GS3 profiles included organic matter content, total carbon (TC), total organic carbon (TOC), total N (TN), total S (TS), selected metal (Na, K, Ca, Mg, Fe, Mn, Cu, Zn) and Hg content determinations. The analyses were based on a total of 181 samples from the GS1 profile, and further 171 samples from the GS3 profile. All samples for geochemical analyses, performed at the Institute of Marine and Environmental Sciences (University of Szczecin) facilities were freeze-dried in Beta 1–8 LDplus laboratory freeze-dryer (Martin Christ) and homogenized using an agate mortar and pestle. Concentrations of selected biogenic elements (TC, TN, and TS) were determined in a Vatio Max CNS Element Analyzer (Elementar). TOC was determined in a Rapid CS Cube (Elementar). The organic matter content was determined via loss on ignition at 550 °C, following the protocol described by Heiri et al. (2001). The organic matter-deprived ash remaining after sediment combustion was treated with 8 ml of concentrated nitric acid, 2 ml of 10% hydrochloric acid, and 2 ml of hydrogen peroxide in a Speedwave microwave mineraliser (Berghof). Atomic absorption spectrometry assays of the solutions obtained to reveal their content of Na, K, Ca, Mg, Fe, Mn, Cu, and Zn were conducted using an AAS SOLAAR 969 spectrometer (Unicam). Mercury (Hg) concentrations were measured using a Direct Mercury Analyser DMA-80 (Milestone), with all samples analyzed in triplicate, and a mean value calculated from these results. The relative error in measuring the content of each element is 1.5–3%. Geochemical analyses were performed in the

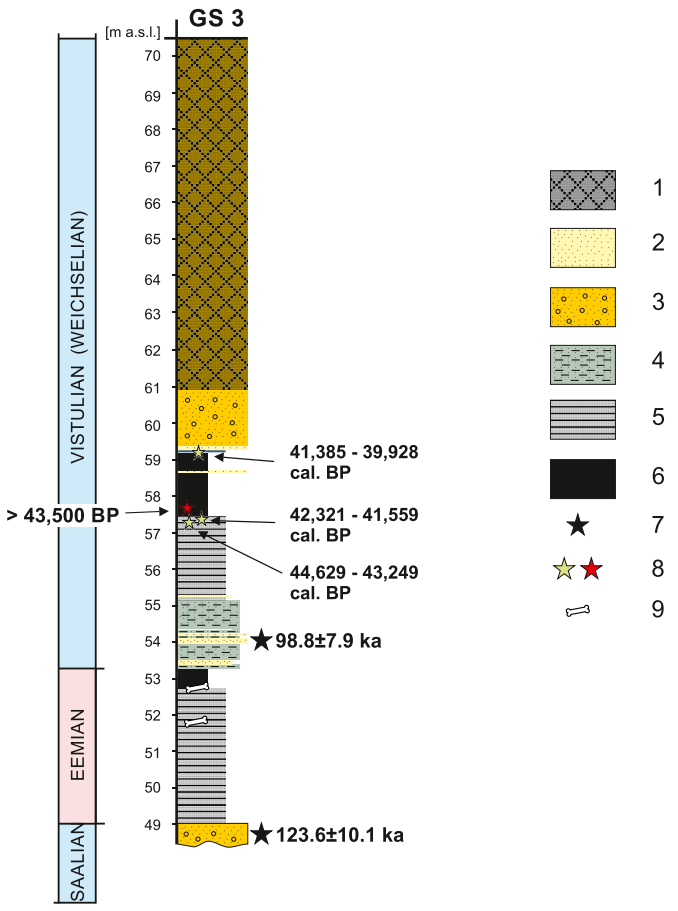


**Fig. 3.** Lithology and results of dating of the sediments from the GS3 profile. 1 – Vistulian till with mixed sands and gravels; 2 – fine and medium grain sand; 3 – unsorted sand mixed with gravel; 4 – silty sand; 5 – calcareous gyttja; 6 – peat; 7 – OSL age ka BP (after Sobczyk et al., 2020); 8 – calibrated median radiocarbon age, in red –data discarded (see Table 2 for details); 9 – bones.

Institute of Marine and Environmental Sciences of the University of Szczecin.

### 3.2. Stable isotopes analyses

The stable isotope analyses included the oxygen and carbon isotope analysis of carbonate sediments and the carbon and nitrogen analysis of the organic matter. Analyses for oxygen and stable carbon isotopes were performed on 183 (103 samples from GS3 and 80 – from GS1) samples of carbonate sediments, using the classical phosphoric acid method (McCrea, 1950). The isotopic compositions were measured using a Finnigan MAT Delta + gas spectrometer. The oxygen and carbon isotope ratios are presented in standard delta notation ($\delta^{18}O_{carb}$, $\delta^{13}C_{carb}$) versus the V-PDB standard and are presented in the form of curves of variation of $\delta^{18}O_{carb}$ and $\delta^{13}C_{carb}$. The analytical error was ±0.1‰ for $\delta^{18}O_{carb}$ and ±0.05‰ for $\delta^{13}C_{carb}$.

Analyses for carbon and nitrogen isotopes were performed on 195 (165 samples from GS3 and 30 – from GS1) samples of organic matter excavated from carbonate sediments and silty sands, and on peat. The sediments were dried at 60 °C and ground. The carbonate fraction was removed with hydrochloric acid. The carbon and nitrogen isotope compositions were analyzed using a Flash Elemental Analyzer 1112 and a Thermo MAT 253 mass spectrometer, which were calibrated based on an internal nicotinamide standard and reported as per mill (‰) deviations versus atmospheric N2 ($\delta^{15}N$) and Vienna Pee Bee Belemnite ($\delta^{13}C_{org}$). The carbon and nitrogen isotope ratios are presented in the form of curves of variation of $\delta^{13}C_{org}$ and $\delta^{15}N$. The analytical errors (1 SD) for the $\delta^{13}C_{org}$ and $\delta^{15}N$ measurements were 0.17‰ and 0.24‰, respectively. Isotopic analyses were performed in the Stable Isotope Laboratory in the Institute of Geological Sciences of the Polish Academy of Sciences in Warsaw, Poland.

### 3.3. Chronology

The chronology of the studied sediments was based on the results of luminescence (OSL) and radiocarbon ($^{14}C$, AMS) datings according to Sobczyk et al. (2020) and three new radiocarbon $^{14}C$ datings performed from the top of upper limnic layers within the GS3 profile (Table 2, Fig. 3). Plant macrofossils were dated by the AMS method by Beta Analytic radiocarbon dating laboratory (Miami, USA).

**Table 1**
Correlation of the stratigraphic units of the Upper Pleistocene in Poland and Western Europe.

| WESTERN EUROPE (after Behre and Lade (1986); van der Hammen (1995) | | | POLAND (after Marks et al., 2016) | | MIS |
|---|---|---|---|---|---|
| HOLOCENE | | | HOLOCENE | | 1 |
| VISTULIAN (=WEICHSELIAN) | Late Pleniglacial | Late Glacial | Late Vistulian | | 2 |
| | | Mecklenburg | Upper Plenivistulian | Gardno | |
| | | Pomeranian | | Pomeranian | |
| | | Frankfurt | | Poznań | |
| | | Brandenburg | | Leszno | |
| | | Denekamp | Middle Plenivistulian (Interpleni-vistulian) | VS 4 | 3 |
| | | Huneborg | | | |
| | Middle Pleniglacial | Hengelo | | | |
| | | Hasselo | | | |
| | | Moershoofd | | | |
| | | Lattrop | | | |
| | | Glinde | | | |
| | | Ebersdorf | | | |
| | | Oerel | | | |
| | Early Pleniglacial | Schalkholz | Lower Plenivistulian | VS 3 | 4 |
| | Early Glacial | Odderade | Early Vistulian | Rudunki | 5a |
| | | Rederstall | | VS 2 | 5b |
| | | Brörup | | Brörup | 5c |
| | | cooling | | | |
| | | Amersfoort | | | |
| | | Herning | | VS 1 | 5d |
| EEMIAN | | | EEMIAN | | 5e |
| SAALIAN | | | ODRANIAN + WARTANIAN | | 6 |

**Table 2**
Results of radiocarbon dating, ages calibrated using IntCal20 approach (Reimer et al., 2020). Explanations for abbreviations: m a.s.l. (metres above sea level); m b.s.l. (metres below surface level). Abbreviations: a – delta 13C values were measured separately in an IRMS (isotope ratio mass spectrometer); N/A – data not available.

| Sample number | Laboratory code | Sampling altitude (m a.s.l.)/ depth (m b.s.l.) | Geological context | Dated material | Conventional age, years BP | Cal 1 sigma years BP (95%) | delta $^{13}$C (‰ VPDB) |
|---|---|---|---|---|---|---|---|
| GS3-GOR4 | Beta–596601 | 56.26/11.90–11.95 | Upper gyttja | *Carex* sp. biconvex – 2 fruits<br>Tissue of plants – 10 fr. | 41,120 ± 370 | 44,629–43,249 | −19.1[a] |
| GS3-139095 | Beta–582623 | 57.55/13.90–13.95 | Upper peat | *Carex rostrata* – 4 fruits<br>*Eleocharis palustris* – 1 fruit<br>Brown moses – 1 stalk<br>*Carex* sp. – 2 fruits | 37,380 ± 320 | 42,321–41,559 | −23.5[a] |
| GS3-141015 | Beta–582624 | 57.67/14.10–14.15 | Upper peat | *Carex rostrata* – 25 fruits<br>*Eleocharis palustris* – 1 fruit<br>Brown moses – 1 stalk | >43,500 | N/A | −25.1[a] |

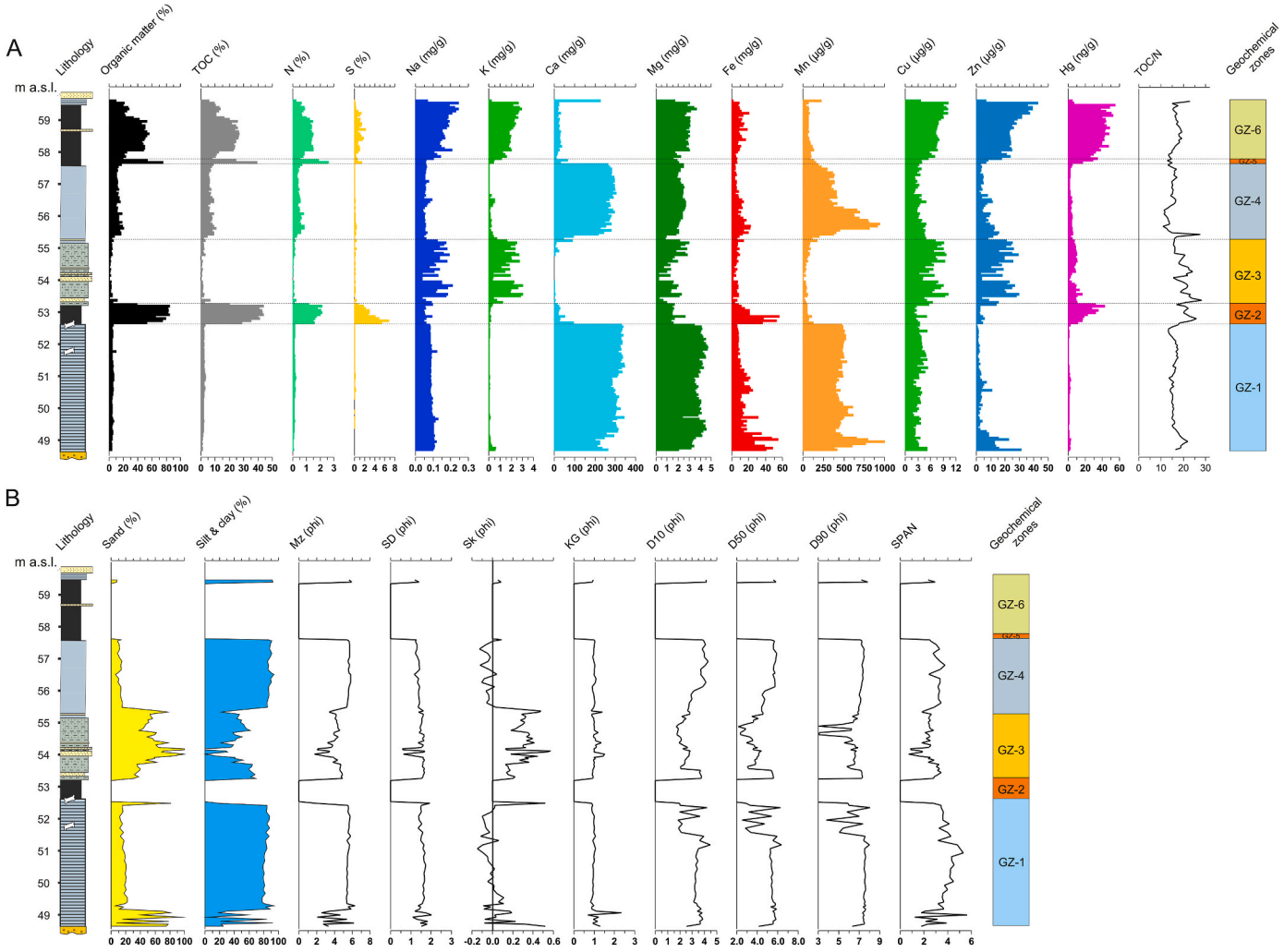


**Fig. 4.** Results of geochemical (A) and grain size (B) analyses of sediments from the GS3 profile. Mz, SD, Sk, Kg – basic statistical parameters according to Folk and Ward (1957); D10, D50, D90 – percentile particle size data; SPAN – dimensionless sorting index according to Foster et al. (2008), obtained by the following formula [(D90-D10)/D50].

## 4. Results

### 4.1. Geochemistry

Geochemical results for GS3 and GS1 profiles are presented in Figs. 4 and 5. These data indicate that GS1, located in the marginal part of the examined sedimentary basin is correlative only to the lower part of GS3, comprised of carbonate sediments of an older lacustrine basin.

#### 4.1.1. GS3 profile

Six geochemical zones (GZ1–GZ6) were distinguished based on the variations in chemical composition of sediments from the GS3 profile. These zones distinctly differ in lithology, and concentrations of biogenic elements, metals, and mercury (Fig. 4):

**GZ-1** zone is a 4 m-thick series of calcareous gyttja. It is characterized by low organic matter (ca. 5%), TOC, TN, and TS, as well as K and Hg (Table 3). It is, however, rich in Ca (ca. 305 mg/g), Mg (ca. 4 mg/g), and Mn (ca. 523 mg/g), and an up section decrease in Fe and Zn contents. In the basal part of this zone, especially below 49.2 m a.s.l., low concentrations of Ca and Mg are associated with maximum concentrations of Fe, Mn, and Zn, and high K contents. Notably, Hg concentrations are somewhat higher in the basal (49.0–48.7 m a.s.l.) and middle (51.0–50.5 m a.s.l.) parts of the GZ-1 zone.

**GZ-2** zone is a 0.6 m-thick peat layer. It displays peak organic matter, TOC, TN, and TS concentrations, and high Fe and Hg concentrations. There is a gradual up section increase in Hg concentrations, from 10 to 40 ng/g, respectively. Fe and S concentrations are the highest at the base of the peat layer (Fig. 4).

**GZ-3** zone is a ca. 2 m-thick series of silty-sandy sediments, with a variable but a generally high proportion of psammitic fraction, in some levels comprising up to 80–90% (Sobczyk et al., 2020). Organic matter and biogenic element contents are at minimum levels. Although strongly variable, generally high concentrations of lithophilous elements (Na, K, Mg) and Cu and Zn are observed within the GZ-3 zone. Hg concentration varies from 1.3 to 16.6 ng/g, with an average of 8.3 ng/g.

**GZ-4** zone is a 2.2 m-thick series of calcareous gyttja. Compared to the lower calcareous gyttja layer (GZ-1), it shows twice as high organic matter concentrations (ca. 13.3%), and a distinctly higher content of biogenic elements (Table 3). Concentrations of Ca and Mg are slightly lower, however. Notably, in the basal part of this zone, from 56.7 to 55.4 m a.s.l., Mn, Fe, Cu, and Zn concentrations are distinctly higher. K and Hg concentrations are elevated in this zone as well.

**GZ-5** zone is thin, ca. 0.1 m-thick peat layer containing 54–76% organic matter and on ca. 31.9% TOC, ca. 2.2% TN, and ca. 1% TS (Table 3). Hg concentration within this zone reaches 29 ng/g.

**GZ-6** zone is a series of mixed organic and mineral sediments, which display both elevated organic matter and biogenic element concentrations (TOC, TN, TS), and high content of lithophilous elements (Na, K, Mg). Cu, Zn, and Hg concentrations increase up section (Fig. 4). Na, K, Cu, Zn, and especially Hg reach the highest average values in this zone (Table 3).

#### 4.1.2. GS1 profile

GS1 profile is located in the marginal, southern part of the sedimentary basin. Within the interval comprised between 50.9 and 40.0 m a.s.l., the GS1 profile is composed of rather uniform calcareous gyttja that is equivalent to zone GZ-1 in profile GS3. Organic matter content ranges from 1.9 to 10.9% (ca. 4.8% – Table 3). Average concentrations of TOC, TN, TS, and K, and Hg are low (Table 3). In the basal part of the GS1 profile composed of the calcareous gyttja layer, we observe elevated concentrations of K, Fe, Mn, Zn, and Hg, and slightly lower concentrations of Ca and Mg, similar to the GZ-1 zone of GS3 profile (Figs. 4 and 5). Immediately superjacent to the calcareous gyttja is a thin, 0.1 m-thick (51.0–50.9 m a.s.l.) organic layer that is correlative to the GZ-2 zone in profile GS-1. Compared to the subjacent gyttja, the organic layer displays elevated concentrations of organic matter, TN and TS, as well as Na, K, Fe, Zn, and Hg. The highest Hg concentration (108 ng/g), however, is observed in the topmost interval of the calcareous gyttja, at ca. 50.8 m a.s.l.

### 4.2. Stable isotopes

The isotope records of the GS3 and GS1 profiles from the succession in Gorzów Wielkopolski site are generally similar. The observed alterations resulted from the location of the studied profiles in different parts of the lake, where various sedimentological processes took place.

#### 4.2.1. GS3 profile

The values of $\delta^{18}O_{carb}$ change from −10.7‰ to −4.9‰, and $\delta^{13}C_{carb}$ values oscillate between −4.1‰ and 12.0‰ (Fig. 6). In the GZ-1 zone, the lowest deposits (below the 48.7 m a.s.l.), consisting of calcareous detritus gyttja have the lowest values of $\delta^{18}O_{carb}$ (from −10.7 to −7.8‰) as well as lowest values of $\delta^{13}C_{carb}$ (from −4.1 to −3.5‰). The oxygen and carbon isotopes reach their minima in the entire profile. In the overlying sediments (to ca. 49.6 m a.s.l.), the values of $\delta^{18}O_{carb}$ abruptly increase and strongly fluctuate from −6.1 to −5.1‰. At that time the carbon isotope values increase from −4.1 to −3.1‰. The isotopic fluctuations are followed by a decrease of $\delta^{18}O_{carb}$ b to −6.8‰ and even values of ca. −4‰ for $\delta^{13}C_{carb}$. Next to ca. 50.7 m a.s.l., the $\delta^{18}O_{carb}$ values oscillate around −6‰ and the $\delta^{13}C_{carb}$ values slightly rise to ca.

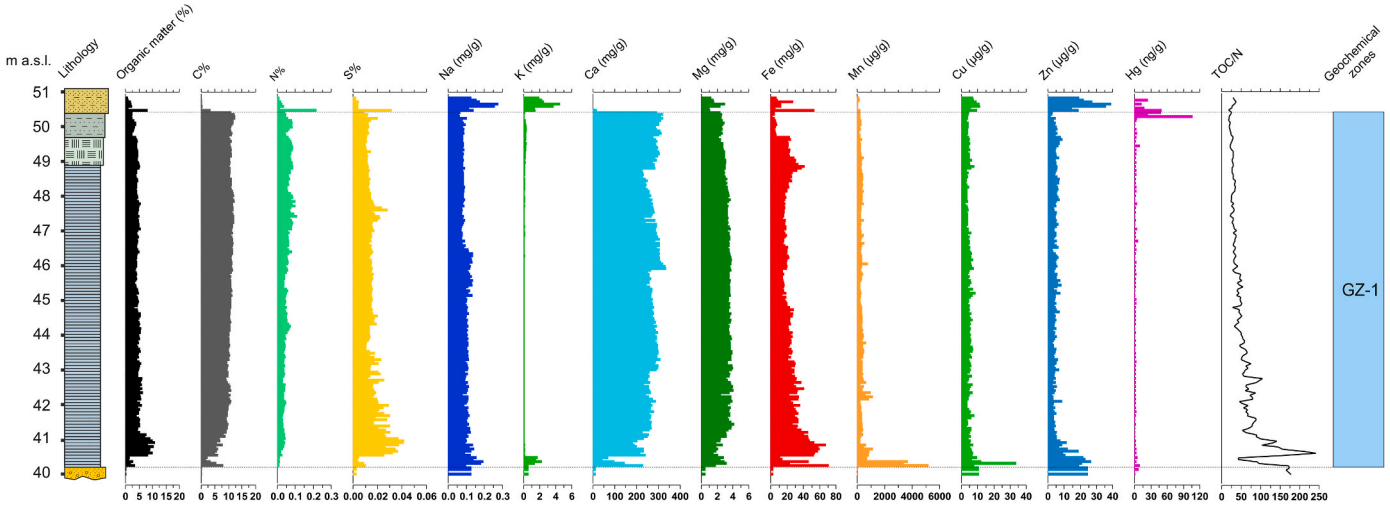


**Fig. 5.** Results of geochemical analyses of sediments from the GS1 profile.

**Table 3**
Average content of organic matter, biogenic elements, metals and mercury in the distinguished geochemical zones of the GS3 and GS1 profiles. * – correlation with GS3 profile.

| GZ | Height (m a.s.l.) | OM (%) | TOC (%) | TN (%) | TS (%) | Na (mg/g) | K (mg/g) | Ca (mg/g) | Mg (mg/g) | Fe (mg/g | Mn (μg/g) | Cu (μg/g) | Zn (μg/g) | Hg (ng/g) |
|---|---|---|---|---|---|---|---|---|---|---|---|---|---|---|
| Profile GS3 | | | | | | | | | | | | | | |
| GZ-6 | 59.6–57.8 | 37.73 | 18.42 | 1.08 | 0.90 | 0.17 | 2.03 | 31.20 | 2.78 | 10.12 | 82.38 | 7.82 | 26.67 | 39.62 |
| GZ-5 | 57.7–57.6 | 64.94 | 31.87 | 2.25 | 1.03 | 0.06 | 0.45 | 50.00 | 2.00 | 6.05 | 143.28 | 3.93 | 7.37 | 23.02 |
| GZ-4 | 57.6–55.4 | 13.30 | 7.06 | 0.49 | 0.17 | 0.06 | 0.16 | 271.53 | 2.27 | 9.71 | 469.47 | 3.44 | 6.81 | 3.55 |
| GZ-3 | 55.3–53.3 | 3.00 | 1.44 | 0.08 | 0.16 | 0.13 | 1.81 | 7.59 | 1.54 | 6.18 | 51.70 | 7.08 | 18.29 | 8.28 |
| GZ-2 | 53.2–52.6 | 72.96 | 38.07 | 1.78 | 3.50 | 0.06 | 0.16 | 34.11 | 1.64 | 28.12 | 69.13 | 3.23 | 4.46 | 25.72 |
| GZ-1 | 52.6–48.7 | 4.99 | 2.13 | 0.14 | 0.08 | 0.10 | 0.09 | 304.71 | 3.95 | 16.45 | 523.55 | 3.45 | 4.49 | 1.33 |
| Profile GS1 | | | | | | | | | | | | | | |
| GZ-1* | 50.9–40.0 | 4.84 | 2.07 | 0.05 | 0.02 | 0.10 | 0.14 | 269.47 | 3.30 | 24.68 | 427.22 | 5.17 | 5.59 | 2.31 |

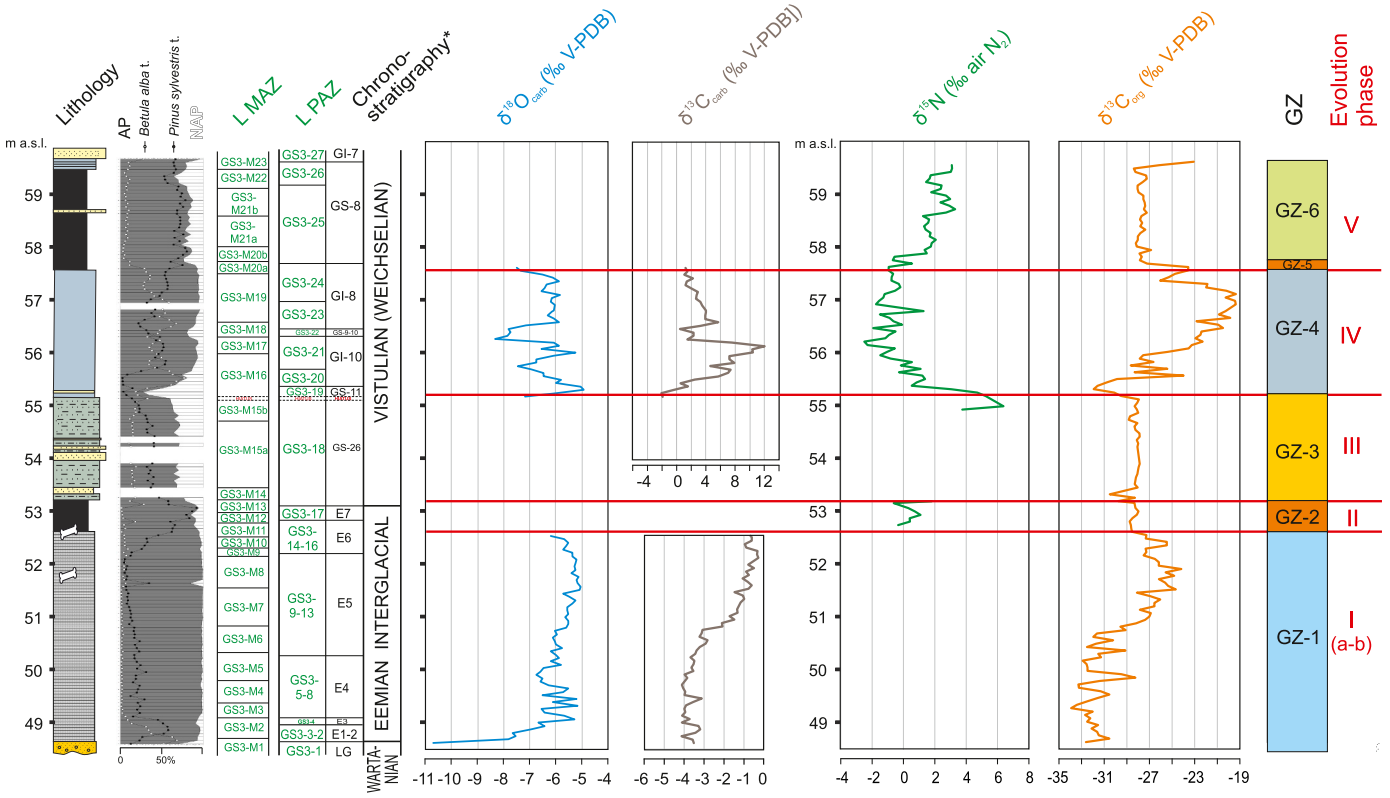


**Fig. 6.** Results of isotope analysis of the sediments from the GS3 profile.
GZ – geochemical zones; LMAZ – local macrofossil assemblage zones; LPAZ – local pollen assemblage zones; * Chronostratigraphy of the EEMIAN INTEGLACIAL – after (Mamakowa, 1989); VISTULIAN (WEICHSELIAN) – after Rasmussen et al. (2014).

−2.8‰. In the overlying sediments (to 51.5 m a.s.l.), $\delta^{18}O_{carb}$ increases to −5‰ and $\delta^{13}C_{carb}$ – to −0.8‰. These increases are interrupted only at ca. 51.4 m a.s.l., by declines in both of oxygen (to −5.5‰) and carbon (−1.5‰) isotope values. Next, the $\delta^{18}O_{carb}$ values are irregular but systematically decrease to −6.2‰. Initially, the $\delta^{13}C_{carb}$ values further increase to −0.3‰ and then, slightly and unevenly drop to −0.8‰. Then calcareous gyttja is replaced by peat (GZ-2 zone) and next by silty sand (GZ-3 zone), and the lack of carbonates makes this isotopic analysis impossible. At 57.6–55.2 m a.s.l. again the carbonate sediments (gyttja) occur (end of GZ-3 and GZ-4). These deposits are characterized by two peaks for the highest values of $\delta^{18}O_{carb}$ of ca. −4.9 and −5.2‰. These increases are separated by a drop to −7.5‰. At that period, the $\delta^{13}C_{carb}$ values irregularly increase to 12‰ and reach maximum values in the entire profile (ca. 56.1 m a.s.l.). Next, $\delta^{18}O_{carb}$ drops to −7.8 to −8.3‰ and $\delta^{13}C_{carb}$ – to 0.5–1.5‰. After rapidly increase to −5.9‰, $\delta^{18}O_{carb}$ fluctuates from −6.5 to −5.8‰. Finally, the oxygen isotope values drop to −7.5‰. The $\delta^{13}C_{carb}$ values also rise to 5.7‰, and then systematically decrease to 1.2‰ (ca. 57.6 m a.s.l.). Next, again the calcareous gyttja is replaced by peat (GZ-5 zone), and the lack of carbonates made this isotopic analysis impossible. Partly a positive correlation of $\delta^{18}O_{carb}$ and $\delta^{13}C_{carb}$ curves occurs, characterizing a closed system of the lake. In such a case, a change of water volume in the lake leads to a change of the isotopic composition of water and precipitated carbonates.

The values of $\delta^{13}C_{org}$ change from −33.9‰ to −19.4‰. In the lower layer of carbonate sediments and silty sands, the content of nitrogen is very low, therefore the nitrogen isotope values can't measure. In upper layers of sediments, $\delta^{15}N$ values fluctuate between −2.5 and 6.4‰ (Fig. 6). In the lowest deposits (below the 48.7 m a.s.l.), $\delta^{13}C_{org}$ increases from −32.6 to −30.5‰. Then, the $\delta^{13}C_{org}$ values irregularly drop −33.9‰ and reach the minimum of values in the entire profile (at 49.3 m a.s.l.). Next (to 49.8 m a.s.l.), a two-steps increase in $\delta^{13}C_{org}$ values ca. −28.2‰ is followed by a briefly drop to −32.9‰. Then the carbon isotope values irregularly increase to −24.2‰ (at 51.9 m a.s.l.). Next (to 53.3m a.s.l.), $\delta^{13}C_{org}$ decreases to −30.5‰. In the silty sands (55.1–53.4

m a.s.l.), the $\delta^{13}C_{org}$ values oscillate around −28‰. In the overlying sediments, the $\delta^{13}C_{org}$ values initially briefly decrease to ca. −32‰, and then two-steps increase to ca. −24‰ and to −19.4‰ (maximum of values). Next, they drop to −27.9‰. In the upper organic deposits (59.5–57.7 m a.s.l.), the $\delta^{13}C_{org}$ values slightly oscillate between −27 and −28‰. In the uppermost deposits, $\delta^{13}C_{org}$ again increases to −23.1‰. In the lower peat layer, the $\delta^{15}N$ values fluctuate from −0.6 to 1.8‰ (53.2–52.7 m a.s.l.). Next, the $\delta^{15}N$ values reach a maximum of values of 6.4‰. This increase is followed by a large decline to −2.5‰ (minimum of values). Next, the $\delta^{15}N$ values irregularly, three-steps increase to1.3‰, 2.1‰, and 3.3‰ (at 58.7 m a.s.l.). Then, they decrease to ca. 1.4‰, and again increase to ca. 3‰.

#### 4.2.2. GS1 profile

The values of $\delta^{18}O_{carb}$ oscillated between −7.0‰ and −5.8‰, and $\delta^{13}C_{carb}$ values changed from −4.8‰ to 0‰ (Figs. 7 and 8). The analyzed deposits consist of calcareous detritus gyttja. In the lowest part of the GS1 profile (43.5 m a.s.l.), the oxygen and carbon isotopes reached even and fairly low values. The $\delta^{18}O_{carb}$ oscillated around ca. −6.5‰ and $\delta^{13}C_{carb}$ fluctuated from −4.8 to −3.8‰. In the overlying sediments (to ca. 46.9 m a.s.l.), the values of $\delta^{18}O_{carb}$ slightly increased to ca. −6‰ (only at 46.1 m a.s.l. they reached values of −5.8‰) and $\delta^{13}C_{carb}$ systematically rose to −2.2‰. The isotope curves show a positive correlation, suggesting a closed lake system. In this case, the change in the water volume in the lake leads to a change in the isotopic composition of the water and precipitated carbonates. Then the oxygen isotope values oscillated around ca. −6‰ (to 47.7 m a.s.l.). At that time the carbon isotope values fluctuated from −2.7 to −2.2‰). The isotopic fluctuations were followed by a several-degree decrease of $\delta^{18}O_{carb}$ to −6.9‰ and even values of ca. – 2.3‰ for $\delta^{13}C_{carb}$. Next to ca. 50.0 m a.s.l., the $\delta^{18}O_{carb}$ values initially increased to −5.8‰ (maximum of the oxygen isotope values) and then fast dropped to −6.9‰.The $\delta^{13}C_{carb}$ values slightly rose to ca. −1‰. In the top of carbonate sediments (to 50.7 m a.s.l.), increases in the $\delta^{18}O_{carb}$ values to −6‰ and in the $\delta^{13}C_{carb}$ values – to 0‰ were observed. These increases were interrupted only at ca. 50.2 m a.s.l., by declines in both oxygen (to −6.5‰) and carbon (−1.3‰) isotope values. The carbonate sediments ended by the $\delta^{18}O_{carb}$ values of −6.7‰ and the $\delta^{13}C_{carb}$ values of 0‰. Then calcareous gyttja was replaced by peat and next by silty sand, and the lack of carbonates made this isotopic analysis impossible.

The analyses of carbon and nitrogen isotopes were performed on organic matter excavated from carbonate-rich sediments from the upper part of the GS1 profile. The content of nitrogen was very low, therefore the nitrogen isotope values couldn't measure. The values of $\delta^{13}C_{org}$ changed from −32‰ to −25.5‰ (Fig. 7). In the deposits to a height of 47.3 m a.s.l., the $\delta^{13}C_{org}$ values increased in two steps from −30.5 to −28.5 and then to −27.1‰. Next, the $\delta^{13}C_{org}$ values dropped −31.8‰ (at 48.9 m a.s.l.). Then the $\delta^{13}C_{org}$ values oscillated around −31‰, and finally reached the minimum of values in the entire profile of −32‰ (at 50.0 m a.s.l.). Then a two-steps increase in $\delta^{13}C_{org}$ values ca. −28.2‰ was followed by a brief drop to −32.9‰. Then the carbon isotope values quickly increased to maximal values of −25.5‰ (at 50.5 m a.s.l.). In the upper organic deposits (to 51.1 m a.s.l.), $\delta^{13}C_{org}$ values dropped to −28‰ and then oscillated around −27‰.

### 4.3. Chronology

Three new radiocarbon $^{14}C$ AMS measurements have been performed for plant macrofossils derived from the lowest part of the upper peat and the topmost of the upper gyttja horizons (Table 2). The sample GS3-GOR4 collected at the top of gyttja level revealed a 44,629–43,249 cal BP radiocarbon age. The GS3-139095 collected at the bottom of peat level revealed 42,321–41,559 cal BP radiocarbon age. The sample GS3-141015 from the central part of peat horizon has an open system characteristic (age >43,500 BP), thus was discarded from further interpretation (red star on the Fig. 3). New $^{14}C$ dating obtained for the sample

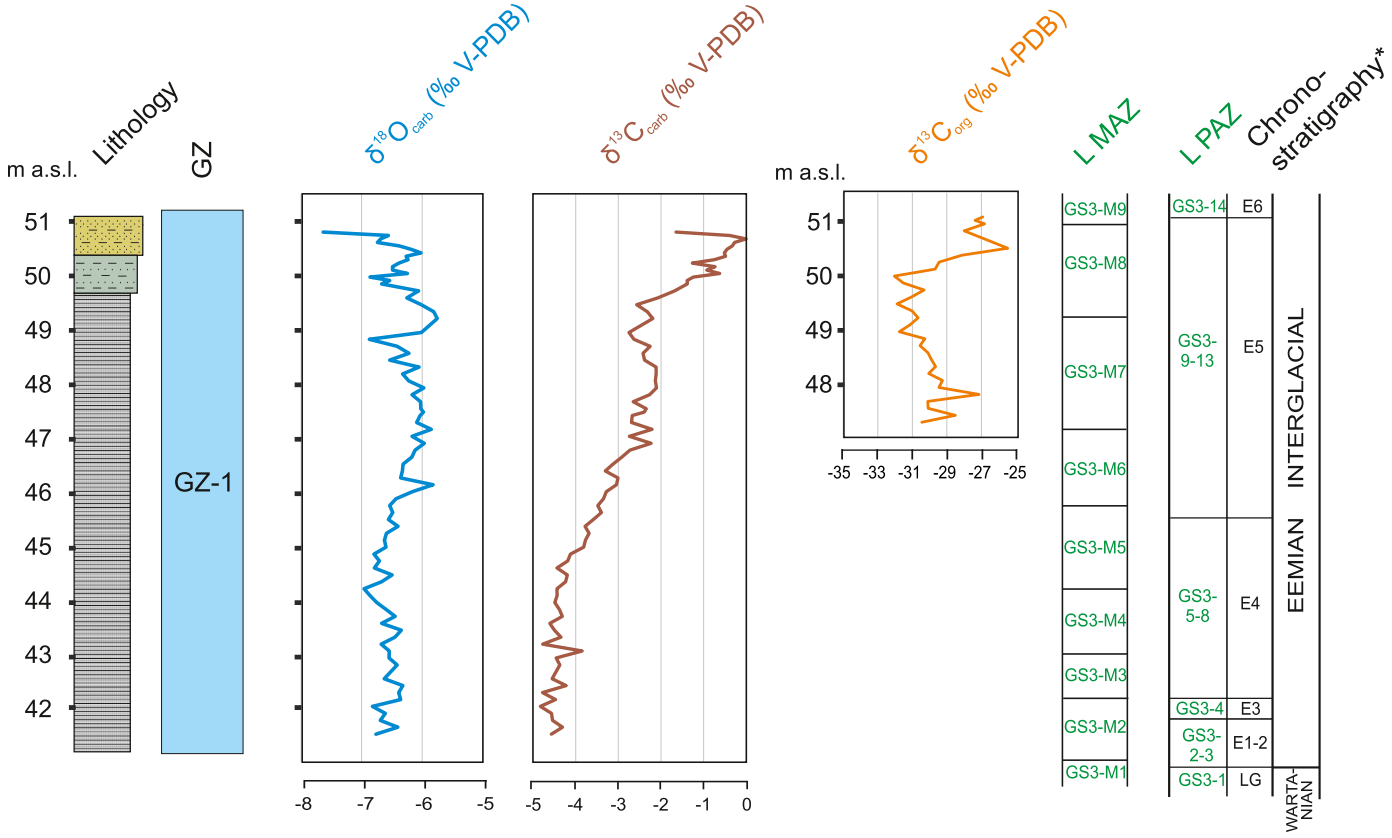


**Fig. 7.** Results of isotope analysis of the sediments from the GS1 profile. GZ – geochemical zones. See Fig. 6 for the other legend.

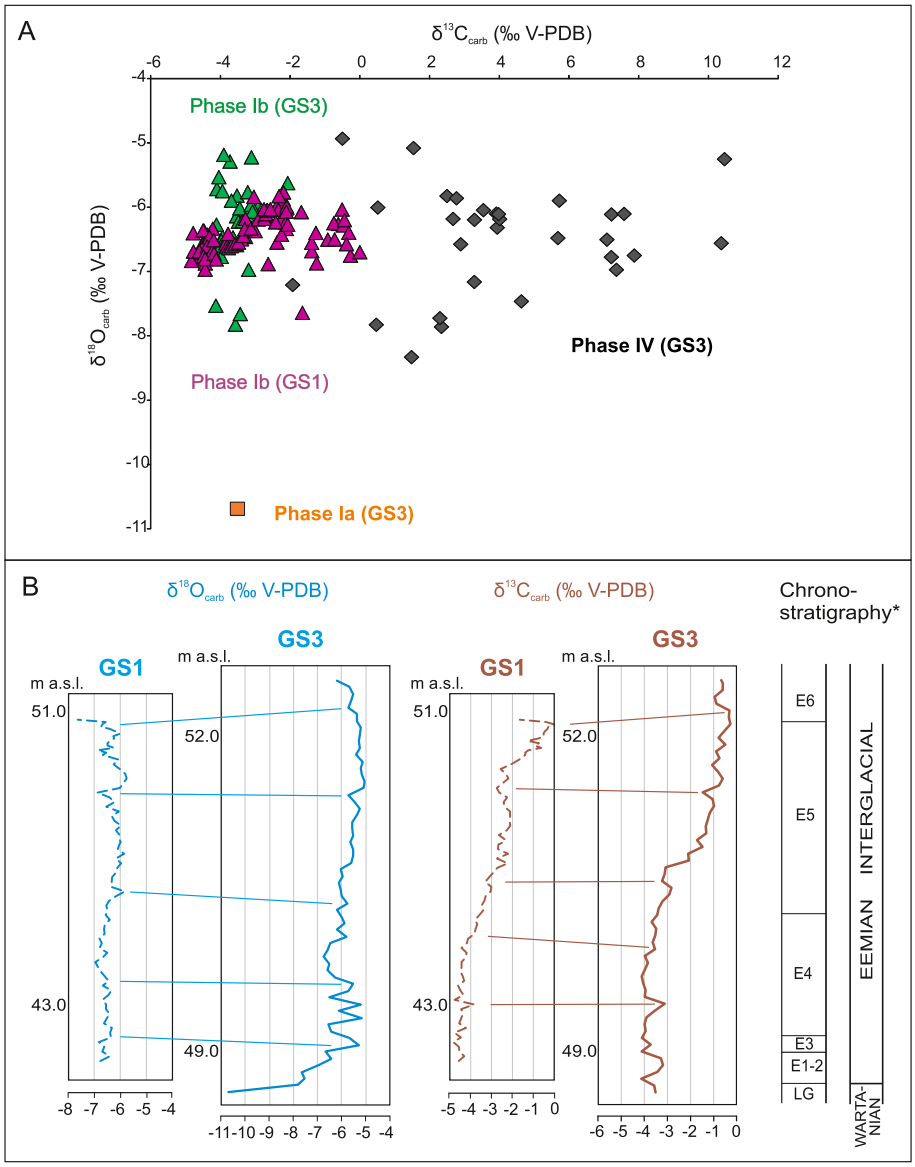


**Fig. 8.** Comparison of the isotope data of the GS1 and GS3 profiles. A: Co-variation between the $\delta^{18}O_{carb}$ and $\delta^{13}C_{carb}$ values of GS1 and GS3 profiles. B: Correlation between the GS1 and GS3 profiles.

derived from the upper peat horizon (Table 2) indicates a continuous record of an overgrown lake between ca. 42–40 ka cal BP replacing the accumulation of gyttja at least 42–44 ka cal BP.

The age of the silt-sand sediments separating the two limnic layers, as is the age of the sediments occurring at the bottom of the lower limnic layer was determined on the basis of optically simulated luminescence datings (OSL). Geochronological investigations performed for quartz-bearing glaciofluvial sediments sandwiching palaeolakes horizons at GS3 locality revealed a tight cluster of OSL central ages between 123.6 ± 10.1 and 98.8 ± 7.9 ka (Sobczyk et al., 2020). The older OSL age points out to the latest phase of fluvial deposition during the Wartanian (Saalian) Glaciation, the younger one marks the transition from warmer Eemian to colder Vistulian (Weichselian) conditions.

Due to the diverse lithology of the studied sediments and the resulting necessity to use different dating methods, it was impossible to reconstruct a reliable age-depth model or to determine the deposition rate of the analyzed sediments.

## 5. Discussion

We used the geochemical and isotopic data to recognize the main five phases of evolution of the palaeolake(s) at Gorzów Wielkopolski site (Fig. 9).

### 5.1. Phase I – lake development during the final phase of the Wartanian (Late Saalian, MIS 6) – Early and Middle Eemian (MIS 5e)

The palaeolake at Gorzów Wielkopolski site originated in the final phase of the Wartanian (Late Saalian) Glaciation. Following deglaciation, a lake basin formed as a narrow melt-out depression in the ground moraine area. The mainly glaciofluvial sands and gravel occurred on the bottom – subphase Ia (Badura et al., 2017; Sobczyk et al., 2020). The lacustrine succession started by carbonate gyttja (lower limnic layer) – subphase Ib. The bottom-most lacustrine sediments are characterized by a high content of $CaCO_3$ to above 80%. There the lowest $\delta^{18}O_{carb}$ values below −7.5‰ are noted (Fig. 6). The lowest $\delta^{18}O_{carb}$ values are related to the isotopic composition of lake water enriched in the light $^{16}O$ isotope, originating likely from melting dead ice blocks. The

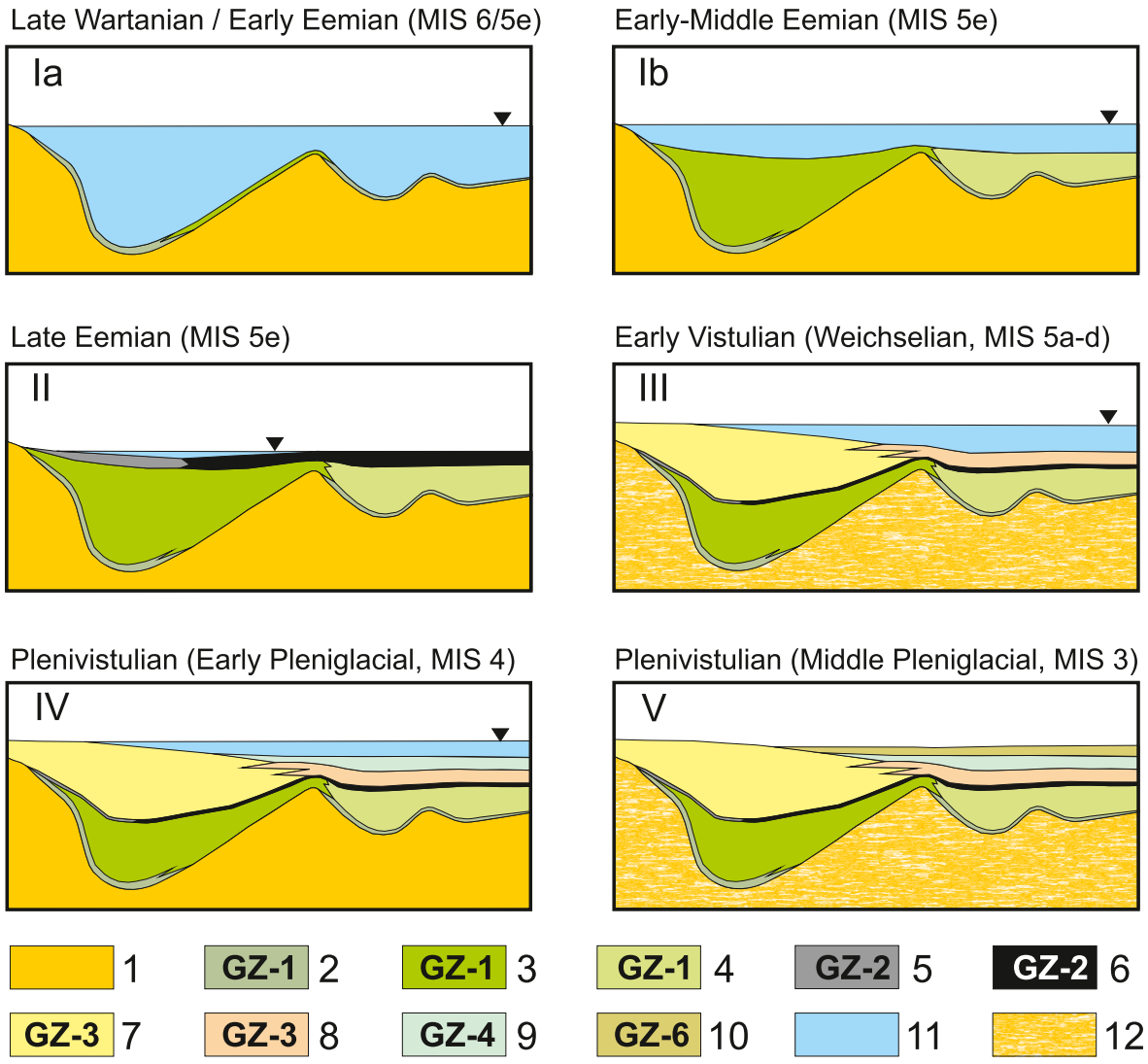


**Fig. 9.** Evolution phases of the palaeolake(s) at Gorzów Wielkopolski.
1 – sand and gravel; 2 – sandy calcareous gyttja; 3 – red-brown calcareous gyttja; 4 – grey calcareous gyttja; 5 – fossil soil; 6 – peat; 7 – delta sand; 8 – silty sand with organic intercalations; 9 – calcareous gyttja; 10 – peaty and detritus gyttja with mineral matter admixture; 11 – lake water; 12 – permafrost; GZ – geochemical zones.

geochemistry data reflect the intensification of mineral matter delivery to the lake basin (Fig. 4B) due to the onset of permafrost degradation and Ca-rich groundwater influx to the lake (Sobczyk et al., 2020). In this period, the palaeolake is fed also by surface waters, although to a minor extent. This is indicated by an elevated content of K, which usually migrates passively, along with clay minerals supplied from surface runoff. This is also corroborated by the granulometry of sediments making up the basal part of the calcareous gyttja (Fig. 4B; Sobczyk et al., 2020). Distinctly higher Zn content in the basal interval of the calcareous gyttja (Figs. 4A and 5) is most likely associated with plant bioaccumulation, especially from then-dominant birch, which is noted for its high bioaccumulation capability concerning zinc (Fortescue, 1980; Adriano, 1986; Reiman et al., 2007). Thus, the presence of Zn in lacustrine sediments may also indicate organic matter and mineral sediment influx from the palaeolake surrounding.

During this phase I, small quantities of organic carbon and nitrogen were detected in the deposits (Figs. 4A and 5). A slightly higher content of organic matter was observed only in the coastal part of the palaeolake (GS1 profile). The organic matter was characterized by a high value of TOC/N (above 20; Fig. 5) and $\delta^{13}C_{org}$ values below −30.5‰. The TOC/N ratio indicates a higher plant component in the sediments (with simultaneous a low primary production) and the low $\delta^{13}C_{org}$ values may reflect the dominance of C3 plants in the catchment. These isotopic and geochemical data suggest that the organic matter presence was caused by the small supply from the land. The isotopic and geochemical record (terrestrial material, low primary production) corresponds with botanical data and suggests an accumulation of these deposits in the final phase of Wartanian (Saalian) Glaciation and at the beginning of the Eemian Interglacial (MIS 6/MIS 5e), under cold, dry climatic conditions. At that time the landscapes were dominated by steppe communities with Poaceae and *Artemisia* and tundra with *Betula nana* and Cyperaceae (GS3-1 NAP-*Betula nana* LPAZ, Sobczyk et al., 2020). In the lake, the vegetation was dominated by Characeae, preferring clear water rich in calcium carbonate (GS3-M1 LMAZ; Sobczyk et al., 2020).

At the beginning of the Eemian Interglacial, a positive trend is noted in $\delta^{18}O_{carb}$ values and as well as in $\delta^{13}C_{carb}$ values of lake carbonates. This tendency results from gradual warming observed in vegetation by the development of bright and open birch (GS3-2 *Betula* LPAZ, E1 RPAZ) and after birch-pine forests with an admixture of *Ulmus*, and a decrease in the share of herbaceous vegetation (GS3-3 *Pinus-Ulmus* LPAZ, E2 RPAZ; Sobczyk et al., 2020). At that time the $\delta^{18}O_{carb}$ values increase by ca. 2–3‰ and the $\delta^{13}C_{carb}$ values rise of ca. 1‰. The low carbon isotopic values of precipitated carbonates (ca. −4‰) suggest a high level of oxygenation in the water, which favored Fe and Mn precipitation

(Fig. 4). Under conditions with insufficient oxygen content, anaerobic conditions may arise in which methanogenesis takes place. In addition an increase of $CaCO_3$ and Mg content is observed. The high $CaCO_3$ content can be interpreted as a consequence of higher warm-related evaporation and carbonate precipitation TOC/N rapidly falls and remains at a level of about 15 (Sobczyk et al., 2020). The lower TOC/N ratio suggests a significant proportion of algae in the organic matter. This finding is confirmed by a decrease in $\delta^{13}C_{org}$ below −31‰ (Fig. 6). The $\delta^{13}C_{org}$ values less than −26‰ are typical for freshwater algae (Leng et al., 2005). Next, the strongly changing $\delta^{18}O_{carb}$ values (to 1.5‰) probably indicate the intense fluctuations in water level (variable ratio of evaporation/precipitation) in the GS3 profile, where shallow-water conditions prevailed, as indicated by the morphology of the palaeolake bed (Sobczyk et al., 2020) and malacofaunal assemblages (Alexandrowicz et al., 2021). In the GS1 profile, in the coastal, but a considerably deeper part of the palaeolake, the constant values of $\delta^{18}O_{carb}$ (ca. −6.5‰) show stable hydrological conditions. At that time likely the lake had the greatest depth documented by aquatic vegetation dominated by species with floating leaves, such *Najas marina*, *Nuphar lutea, Brasenia holsatica*, and *Trapa natans* (GS3-4 *Quercus* and GS3-5-8 *Corylus* LPAZs, E3-E4 RPAZs, GS3-M2-5 LMAZ; LMAZ; Sobczyk et al., 2020). The $\delta^{13}C_{carb}$ values were constant in both parts of the basin (Figs. 6–8). Such trends of carbon isotopic ratios may be associated with the continuous photosynthetic activity of phytoplankton and macrophytes. TOC/N remains at a level of about 15 (Fig. 4A). This TOC/N ratio and the mainly $\delta^{13}C_{org}$ values below −31‰ indicate still a significant share of algae in the organic matter in the sediments.

In the climatic optimum of the Eemian Interglacial, the development of oak-hornbeam forests, including *Carpinus betulus, Corylus avellana, Quercus, Tilia platyphyllos,* and *T. cordata*, as well as of riparian forests, mainly represented by *Alnus glutinosa* is interpreted (GS3-5-8 *Corylus* and GS3-9-13 *Carpinus* LPAZs, E4-E5 RPAZs; Sobczyk et al., 2020). At that time, in both studied parts of this palaeolake, initially, the constant values of $\delta^{18}O_{carb}$ (ca. −6‰) show the stable climatic and hydrological conditions and/or the fast rate of sedimentation. The isotopic composition of lake water was invariable thus precipitated carbonates are characterized by similar isotopic values. The relatively high values of $\delta^{18}O_{carb}$ are connected with gradual warming documented by the pollen data. Then, there a steady increase in the value of $\delta^{18}O_{carb}$ (of ca. 1‰) and especially in $\delta^{13}C_{carb}$ values (of ca. 4‰) as well as increasing $\delta^{13}C_{org}$ values are observed (E5 RPAZ). Such a trend may have coincided with an increase in aquatic productivity (Boettger et al., 2000). Probably at that time the process of shallowing the lake began. In the younger half of the Eemian Climatic Optimum (GS3-9–13 *Carpinus* LPAZ, E5 RPAZ), during a transient, a minor decrease in *Picea abies*, *Corylus avellana*, *Quercus*, *Ulmus,* and *Alnus glutinosa* curves, accompanied by an increase in *Pinus silvestris* curve, there was a decrease in Ca, Mg and Mn concentrations, with a concomitant increase in Zn, Fe and – to a lesser extent – K, Hg, and organic matter, TOC, TN and TS (Figs. 4A and 5). All this may point to a diminished groundwater supply to the palaeolake, with a relative increase in the significance of surface runoff, including mineral and organic matter, enabling a passive migration of Hg. At the same time, Fe/Mn ratio values exceeding in some places 50 (see Sobczyk et al., 2020) may point to the periodic occurrence of reducing conditions at the bottom of the palaeolake (Boyle, 2001; Żarczyński et al., 2019; Makri et al., 2021).

Comparing the oxygen and carbon curves can try also to examine the hydrologic relations in the studied basin. Generally, the positive correlation of $\delta^{18}O_{carb}$ and $\delta^{13}C_{carb}$ curves suggest the closed system of the reservoir. Such a system occurred several times in the history of this palaeolake and was recorded in the GS1 and GS3 profiles. During the second half of the Eemian optimum (pollen zone E5) opposed trend of these curves is observed in both GS3 and GS1 profiles. This phenomenon may suggest the opening of a hydrological system and/or existing small isolated reservoirs. At that time a change of inflow and outflow of water could occur.

### 5.2. Phase II – Mire existence during the post-optimum (Late Eemian, MIS 5e)

During the post-optimum of the Eemian, climatic cooling took place, reflected by the disappearance of hornbeam in the forest communities and domination of coniferous forests including *Picea, Abies,* and *Pinus sylvestris* (GS3-14-16 *Picea-Abies-Pinus* LPAZ, E6 RPAZ; Sobczyk et al., 2020) and the end of the Eemian Interglacial further deterioration of climate, reflected in the *Pinus* domination was observed (GS3-17 *Pinus* LPAZ, E7 RPAZ). At that time, probably the water level dropped and the lake transformed into peat bog. The peat replaced calcareous gyttja and the total lack of carbonates made isotopic analysis of carbonates impossible. In both profiles GS1 and GS3 the transition between the lower limnic layer and the layer of organic sediment is very clearly visible (peat layer), which indicates a fairly rapid change in the water level, as well as in the conditions of sedimentation in the basin. Therefore the amounts of organic carbon and nitrogen rise. An increase of the TOC/N ratio to 20–25 and the higher values of $\delta^{13}C_{org}$ documented the terrestrial source of organic matter. At the same time, the Hg concentrations in the peat layer increases to reach a maximum of ca. 43 ng/g in GS3 profile, and ca. 106 ng/g at the boundary between gyttja and the superjacent layer of peat in GS1 profile (Figs. 4 and 5). Such high Hg concentrations in the Holocene mires are usually linked to human impact, but also the degree of peat decomposition, volcanic events, and – indirectly – to climatic changes (Lacerda et al., 1999; Martinez-Cortizas et al., 1999, 2007; Biester et al., 2002, 2006; Roos-Barraclough et al., 2002; Farmer et al., 2009; Zaccone et al., 2009; Allan et al., 2013; Küttner et al., 2014; Pérez-Rodríguez et al., 2015; Talbot et al., 2017). The latest data on Hg cycling in the Arctic and Antarctic regions (Bargagli, 2016; Obrist et al., 2017; Olson et al., 2018, 2019; Jiskra et al., 2019; Pérez-Rodríguez et al., 2019) point to increased Hg concentrations in plants, soils and organic sediments of tundra regions. The study by Olson et al. (2019) indicates that enhanced atmospheric Hg absorption ($Hg_0$) by tundra plants is an important mechanism that buffers the deposition of Hg in the environment. This is accomplished via leaf fall and decay of peat-forming plants, especially of non-vascular vegetation, which is known to absorb the most Hg Olson et al. (2019). Therefore the higher Hg amount likely corroborates the presence of tundra vegetation caused by climatic cooling.

### 5.3. Phase III – Flow-through lake existence during the Early Vistulian (Early Weichselian, MIS 5a–d)

During the Early Vistulian glaciation, climatic cooling led to loosening the vegetation and development of open, herbaceous communities with *Calluna vulgaris* (GS3-18 *Calluna vulgaris*-NAP LPAZ). In the basin, the water level increased, and fine-grained sediments such as silty sands and silts accumulated being diagnostic for the low-flow conditions (Fig. 4B; Sobczyk et al., 2020). Only the mineral sedimentation took place. The high content of lithophilous elements and the highest so-called erosion index (Na + K + Mg/Ca) reflect the more intensive mechanical denudation processes and suggest also a limitation of vegetation cover. Palynological data indicating the co-occurrence of tundra vegetation (i.a. *Betula nana*) and plants requiring higher temperatures (i.a. *Tilia cordata*) suggest redeposition (Sobczyk et al., 2020). The significant fluctuations in Na, K, Mg, Cu, and Zn concentrations (Fig. 4A) indicate variable conditions of organic and mineral sediment accumulation (Fig. 4B). These could also be determined by the differences in sediment grain size (Fig. 4B).

The concentrations of TOC and TN rapidly decrease to their minimum of values and the TOC/N ratio fluctuates between 15 and 25 (Fig. 4A). The values of $\delta^{13}C_{org}$ are constant at approximately −28‰. At the end of this period, the $\delta^{15}N$ values increase to 6‰ reflecting lower nitrogen availability (Talbot and Laerdal, 2000). The data reflect a reduction in primary production and only sporadic input of terrestrial organic matter into the lake (Meyers and Lallier-Vergès, 1999). The

low-variable values of $\delta^{13}C_{org}$ are likely related to low carbon availability. A slightly lower Hg concentration in these sediments (Fig. 4A) is associated with a considerably lower content of organic matter, which is the main carrier of this element. The high abundance of *Conococcum geophilum* in the sandy-silty sediment layer in the GS3 profile indicates (GS3-M13-15b LMAZ) that the palaeolake underwent periodical drying, or – alternatively – that its area underwent significant shifts.

### 5.4. Phase IV – Reactivation of the lake during the lower Plenivistulian (Early Pleniglacial Weichselian, MIS 4)

Next the further climatic cooling led to dominance of herbaceous communities in landscape. Humid habitats were overgrown by communities of dwarf shrub tundra including especially *Betula nana* (GS3-19 NAP LPAZ). The firstly stable, cold climate led to the development of rare pioneering and heliofilous birch forests mixed with herbaceous vegetation (GS3-20 *Betula*-NAP LPAZ) and next variable values of *Pinus* and *Betula* indicate quite stable interstadial climatic conditions, but with a slight warming trend (GS3-21 *Pinus–Betula* LPAZ). There a reactivation of the lake took place and carbonate sediments (gyttja and limnic chalk) accumulated again – upper limnic layer. The content of Ca was high and similar to the lower lake horizons in phase I. Compared to the lowe limnic layer (phase I), these sediments are distinctly higher TOC and TN contents, indicating higher fertility, especially at the beginning of this phase IV. The low Fe/Mn ratio (ca. 20) points to the dominance of oxidizing conditions that are especially conducive to Mn precipitation, higher than in lower limnic layer form phase I, supplied to the lake from groundwaters. At this time, Hg concentration gradually decreases, which could point to an amelioration of climatic conditions. After an initial increase in the $\delta^{18}O_{carb}$ values, two-steps lowering occurred, probably reflecting a cooling and fluctuations of water level in stadial conditions of GS3-22 NAP-*Betula* LPAZ. The next approximation of the oxygen isotope values suggests more stable hydrological conditions in the interstadial phase of GS3-23 *Betula* and GS3-24 *Pinus-Betula-Larix* LPAZs where again, first birch forests and then pine-birch forests indicate an improvement in the climate. The initially highest $\delta^{13}C_{carb}$ values were caused by an increase in biological activity in the closed shallowing lake. The systematic increase in the $\delta^{13}C_{org}$ values also reflects an increase in photosynthesis, because, with enhanced productivity, aquatic plants preferentially take up $^{12}C$ during photosynthesis (Leng and Marshall, 2004). The drop in the $\delta^{13}C_{carb}$ values corroborates a more oxidizing environment.

### 5.5. Phase V – Decline of the lake during the Middle Plenivistulian (Middle Pleniglacial Weichselian, MIS 3)

In the studied lake basin a gradual re-shallowing occurred which is signalized by replacing carbonate sedimentation with organic deposition, and as a result, the lake transformed into a mire. It caused an increase in TOC and TN content as well as TOC/N ratio (Sobczyk et al., 2020). In peats, characterized by a variable mineral matter admixture, increasing concentrations of several elements may indirectly point to deteriorating climatic conditions. Increasing content of lithophilous elements and an increase in erosion index (Na + K + Mg/Ca) point to the onset of increasingly more intensive mechanical denudation processes (Sobczyk et al., 2020), and thus also to decreasing vegetation cover, likely connected with climatic cooling. This is confirmed by the results of the pollen analysis, which indicate that at that time there were stadial conditions with the predominance of herbaceous vegetation and marked by rebedded sporomorps typical for redeposition (GS3-25 *Pinus*-NAP and GS3-26 NAP-*Pinus* LPAZs). The increase in Cu and Zn concentrations is closely correlated with an increase in erosion index, and with K content (Fig. 4A), which indicates the concentrations of these elements are linked to the intensity of mechanical denudation, and with clay matter supply in particular (Fig. 4B). Further, elevated Zn concentrations may also be associated with bioaccumulation of Zn by some tundra plant taxa, including *Betula nana* (Fortescue, 1980; Adriano, 1986; Reiman et al., 2007). An increasing Hg concentration suggests persistent low temperatures characteristic for tundra regions (Bargagli, 2016; Lacerda et al., 2017; Obrist et al., 2017; Olson et al., 2018, 2019; Jiskra et al., 2019; Pérez-Rodríguez et al., 2019). Next, the peat accumulation stopped.

## 6. Conclusions

The investigated sediments come from different parts of the palaeolake basin and correlated very well. They represent two cycles of lake accumulation (two limnic layers), each ended by peat deposition, separated by mineral deposits. The lower and upper limnic layers, despite several similar geochemical features, are records of two separate phases of the lake's functioning. The palynological data suggest that the mineral deposits separating them are not continuous succession, but contain a stratigraphic hiatus.

Six geochemical zones (GZ-1–6) were distinguished based on the variability of the chemical composition. Geochemical and isotopic data show good correspondence with lithological features of deposits as well climatic changes and reflect the changing environmental conditions (redox conditions, variability and intensity of denudation, biological productivity, and fertility of the environment). In the bottom sediments, some influence of the surface supply is visible, indicated by the increased content of lithophilous elements (e.g. potassium), copper and zinc. The limnic layers (GZ-1, GZ-4) are dominated by slow accumulation of carbonates. The higher mercury content (GZ-2, GZ-6) is related to the course of climate change and is the highest during cold periods.

The greatest variations of isotopic values of carbonates occur in the bottom of the lower limnic layer as well in the upper limnic layer, and are connected with the changing environmental conditions in the basin (water level and temperature). The differences in carbon and nitrogen isotope values suggest different sources of organic matter accumulated in the studied basin and varying trophy of the environment.

Five phases of the evolution of the basin (phases I–V) in relation to the scheme of the vegetation development and climatic changes during the Eemian Interglacial and the Vistulian Glaciation were recognized. The lake accumulation began during the final phase of the Late Wartanian (Saalian) Glaciation (MIS 6). Firstly the palaeolake harmonically developed and reached its maximum depth in the Early and Middle Eemian (phase I, MIS 5e). Then (Late Eemian, MIS 5e) palaeolake transformed into the peat bog (phase II). In the Early Vistulian period (beginning of the Early Weichselian, MIS 5d–a), the lake again existed initially as a flow-through lake (phase III) and after that carbonate sediments (gyttja and limnic chalk) accumulated again (phase IV, MIS 4). Finally, during Middle Vistulian (Middle Weichselian, MIS 3), the palaeolake declined and mire developed (phase V).

## Author contributions

Joanna Mirosław-Grabowska and Ryszard Krzysztof Borówka – conceptualization, interpretation of isotope and geochemical analyses, writing the text. Artur Sobczyk – interpretation of datings, description of lithology. Anna Hrynowiecka – interpretation of pollen analysis, palynological division. Renata Stachowicz-Rybka – interpretation of macro remains analysis, macro fossil division. Magdalena Radzikowska – stable isotope laboratory investigations. Joanna Sławińska – chemical elements laboratory investigations. Krzysztof Stefaniak – funding acquisition, faunal data.

## Data availability

Datasets are available in laboratories for specialized study and tests, performed by the co-authors and will be found after the finish of grant No. 0201/2048/18.

## Declaration of competing interest

The authors declare that they have no known competing financial interests or personal relationships that could have appeared to influence the work reported in this paper.

## Acknowledgements

We would like to thank the entire "Stefania project" team for the opportunity to work together. We are grateful to the anonymous reviewers for their critical comments on previous versions of the manuscript. The present research was supported by grant No. 0201/2048/18 financed by the National Science Centre (NCN), Poland. The authors would like to thank Editors and Reviewers for valuable comments on the manuscript.

## References

Adriano, D.C., 1986. Trace Elements in the Terrestial Environment. Springer Verlag, New York, Berlin, Heidelberg, Tokyo, p. 533.

Alexandrowicz, S.W., Alexandrowicz, W.P., 2010. Molluscs of the Eemian interglacial in Poland. Ann. Soc. Geol. Pol. 80, 69–87.

Alexandrowicz, W.A., Skoczylas, S., Sobczyk, A., Stefaniak, K., Kotowski, A., Przybylski, B., Ciszek, D., Badura, J., Urbański, K., 2021. Mollusc faunas of lake deposits in Gorzów Wielkopolski (NW Poland) as an indicator of environmental changes during Eemian and Early Weichselian. Geol.l Q. 65, 36. https://doi.org/10.7306/gq.1605.

Allan, M., Le Roux, G., Sonke, J.E., Piotrowska, N., Streel, M., Fagel, N., 2013. Reconstructing historical atmospheric mercury deposition in Western Europe using: Misten peat bog cores, Belgium. Sci. Total Environ. 442, 290–301. https://doi.org/10.1016/j.scitotenv.2012.10.044.

Badura, J., Ciszek, D., Kotowski, A., Przybylski, B., Ratajczak, U., Stefaniak, K., Urbański, K., 2017. Title in Polish [Remains of rhinoceros (Stephanorhinus sp.) and fallow deer (Dama dama) discovered in Eemian lake sediments in the Gorzów Plain (NW Poland)]. Prz. Geol. 65, 219–226 [in Polish with English summary].

Bargagli, R., 2016. Moss and lichen biomonitoring of atmospheric mercury: a review. Sci. Total Environ. 572, 216–231. https://doi.org/10.1016/j.scitotenv.2016.07.202.

Behre, K., Lade, D., 1986. Eine Folge von Eem und 4 Weichsel-Interstadialen Oerel/Niedersachsen und ihr Vegetationsablauf. Eiszeitalt. Ggw. 36, 11–36.

Biester, H., Kilian, R., Franzen, C., Woda, C., Mangini, A., Schöler, H.F., 2002. Elevated mercury accumulation in a peat bog of the Magellanic Moorlands, Chile (53° S) – an anthropogenic signal from the Southern Hemisphere. Earth Planet Sci. Lett. 201, 609–620. https://doi.org/10.1016/S0012-821X(02)00734-3.

Biester, H., Bindler, R., Martinez-Cortizas, A., 2006. Mercury in mires. In: Martini, I.P., Martinez-Cortizas, A., Chesworth, W. (Eds.), Peatlands: Evolution and Record of Environmental and Climate Changes. Elsevier B.V., pp. 465–478

Bińka, K., Ber, A., Bałuk, A., 2006. Eemian and Vistulian pollen records from the Łomża region (NE Poland). Geol. Q. 50 (4), 437–446.

Boettger, T., Junge, F.W., Litt, T., 2000. Stable climatic conditions in Central Germany during the last interglacial. J. Quat. Sci. 15, 469–473. https://doi.org/10.1002/1099-1417(200007)15:5<469::AID-JQS550>3.0.CO;2-D.

Boyle, J.F., 2001. Inorganic geochemical methods in Palaeolimnology. In: Last, W.M., Smol, J.P. (Eds.), Tracking Environmental Change Using Lake Sediments. Volume 2: Physical and Geochemical Methods. Kluwer Academic Publishers, Dordrecht, Boston, London, pp. 83–141.

Farmer, J.G., Anderson, P., Cloy, J.M., Graham, M.C., MacKenzie, A.B., Cook, G.T., 2009. Historical accumulation rates of mercury in four Scottish ombrotrophic peat bogs over the past 2000 years. Sci. Total Environ. 407, 5578–5588. https://doi.org/10.1016/j.scitotenv.2009.06.014.

Folk, R.L., Ward, W.C., 1957. Brazos River bar: a study in the significance of grain size parameters. J. Sediment. Petrol. 27, 3–26.

Fortescue, J.A.C., 1980. Environmental Geochemistry – A Holistic Approach. Ecological Studies, 35. Springer-Verlag, New York, Heidelberg, Berlin, p. 347.

Foster, I.D.L., Oldfield, F., Flower, R.J., Keatings, K., 2008. Mineral magnetic signatures in a long core from Lake Quarun, middle Egypt. J. Paleolimnol. 40, 835–849.

Heiri, O., Lotter, A.F., Lemecke, G., 2001. Loss on ignition as a method for estimating organic and carbonate content in sediments: reproducibility and comparability of results. J. Paleolimnol. 25, 101–110. https://doi.org/10.1023/A:1008119611481.

Hrynowiecka, A., Żarski, M., Jakubowski, G., Nadachowski, A., Pawłowska, K., Pawłowski, D., Szymanek, M., Nast, D., 2018. Eemian and Vistulian (Weichselian) paleoenvironmental changes: a multi-proxy study of sediments and mammal remains from the Ławy paleolake (Eastern Poland). Quat. Int. 467, 131–146. https://doi.org/10.1016/j.quaint.2016.10.033.

Jiskra, M., Sonke, J.E., Agnan, Y., Helmig, D., Obrist, D., 2019. Insights from mercury stable isotopes on terrestial-atmosphere exchange of Hg(0) in Arctic tundra. Biogeosciences 16, 4051–4064. https://doi.org/10.5194/bg-16-4051-2019.

Kupryjanowicz, M., 2008. Vegetation and climate of the Eemian and early Vistulian lakeland in northern Podlasie. Acta Palaeobot. 48 (1), 1–130.

Kupryjanowicz, M., Fiłoc, M., Kwiatkowski, W., 2018. Was there an abrupt cold climatic event in the middle Eemian? Pollen record from a palaeolake at the Hieronimowo site, NE Poland. Quat. Int. 467, 96–106. https://doi.org/10.1016/j.quaint.2017.04.027.

Küttner, A., Mighall, T.M., De Vleschouwer, F., Mauquoy, D., Martinez-Cortizas, A., Foster, I.D.L., Krupp, E., 2014. A 3300-year atmospheric metal contamination record from Raeburn Flow raised bog, south west Scotland. J. Archaeol. Sci. 44, 1–11. https://doi.org/10.1016/j.jas.2014.01.011.

Lacerda, L.D., Ribeiro, M.G., Cordeiro, R.C., Sifeddine, A., Turcq, B., 1999. Atmospheric mercury deposition over Brazil during the past 30,000 years. J. Braz. Assoc. Adv. Sci. 51, 363–371.

Lacerda, L.D., Turcq, B., Sifeddine, A., Cordeiro, R.C., 2017. Mercury accumulation rates in Caço Lake, NE Brazil during the past 20,000 years. J. S. Am. Earth Sci. 77, 42–50. https://doi.org/10.1016/j.jsames.2017.04.008.

Leng, M.J., Marshall, J.D., 2004. Palaeoclimate interpretation of stable isotope data from lake sediment archives. Quat. Sci. Rev. 23 (7–8), 811–831. https://doi.org/10.1016/j.quascirev.2003.06.012.

Leng, M.J., Lamb, A.L., Marshall, J.D., Wolfe, B.B., Jones, M.D., Holmes, J.A., Arrowsmith, C., 2005. Isotopes in lake sediments. In: Leng, M.J. (Ed.), Isotopes in Palaeonvironmental Research. Springer, The Netherlands, pp. 147–184.

Majecka, A., Balwierz, Z., Forysiak, J., Twardy, J., 2018. Eemian and Vistulian (Weichselian) development of the meltout depression on the watershed between the Mroga and Mrożyca Rivers (Central Poland) based on lithological and pollen analysis. Quat. Int. 467, 79–95. https://doi.org/10.1016/j.quaint.2016.08.012.

Makri, S., Wienhues, G., Bigalke, M., Gilli, A., Rey, F., Tinner, W., Vogel, H., Grosjean, M., 2021. Variations of sedimentary Fe and Mn fractions under changing lake mixing regimes, oxygenation and land surface processes during Late-glacial and Holocene times. Sci. Total Environ. 755 (2), 143418. https://doi.org/10.1016/j.scitotenv.2020.143418.

Mamakowa, K., 1989. Late Middle Polish Glaciation, Eemian and Early Vistulian vegetation at Imbramowice near Wrocław and the pollen stratigraphy of this part of the Pleistocene in Poland. Acta Palaeobot 29, 11–176.

Marks, L., Gałązka, D., Woronko, B., 2016. Climate, environment and stratigraphy of the last Pleistocene glacial stage in Poland. Quat. Int. 420, 259–271. https://doi.org/10.1016/j.quaint.2015.07.047.

Martinez-Cortizas, A., Biester, H., Mighall, T., Bindler, R., 2007. Climate driven enrichment of polutants in peatlands. Biogeosciences 4, 905–911. https://doi.org/10.5194/bg-4-905-2007.

Martinez-Cortizas, A., Ponteverda-Pombal, X., García-Rodeja, E., Nóvoa-Muñoz, J.C., Shotyk, W., 1999. Mercury in a Spanish peat bog: archive of climate change and atmospheric metal deposition. Science 284, 939–942. https://doi.org/10.1126/science.284.5416.939.

McCrea, J.M., 1950. The isotopic chemistry of carbonates and a paleotemperature scale. J. Chem. Phys. 18, 849–857.

Meyers, P.A., Lallier-Vergès, E., 1999. Lacustrine sedimentary organic matter records of Late Quaternary paleoclimates. J. Paleolimnol. 21, 345–372. https://doi.org/10.1023/A:1008073732192.

Mirosław-Grabowska, J., 2008. Reconstruction of lake evolution at Rzecino (NW Poland) during the Eemian Interglacial and Early Vistulian on the basis of stable isotope analysis. Ann. R. Pol. Acad. Sci. 90–92.

Mirosław-Grabowska, J., Niska, M., Roman, M., 2018. Long (MIS 5e–3) environmental history of a paleolake in Central Poland recorded in the succession from Kubłowo. Quat. Int. 467, 26–42. https://doi.org/10.1016/j.quaint.2016.06.027.

Mirosław-Grabowska, J., Niska, M., Sienkiewicz, E., 2009. Evolution of the palaeolake at Ruszkówek (central Poland) during the Eemian Interglacial based on isotopic, cladoceran and diatom data. J. Paleolimnol. 42, 467–481. https://doi.org/10.1007/s10933-008-9297-0.

Niska, M., Mirosław-Grabowska, J., 2015. Eemian environmental changes recorded in lake deposits from Rzecino (NW Poland): Cladocera, isotopic and selected geochemical data. J. Paleolimnol. 53, 89–105. https://doi.org/10.1007/s10933-014-9810-6.

Obrist, D., Agnan, Y., Jiskra, M., Olson, C.L., Colegrove, D.P., Hueber, J., Moore, C.W., Sonke, J.E., Helmig, D., 2017. Tundra uptake of atmospheric elemental mercury drives Arctic mercury pollution. Nature 547, 201–204. https://doi.org/10.1038/nature22997.

Olson, C., Jiskra, M., Biester, H., Chow, J., Obrist, D., 2018. Mercury in active-layer tundra soil of Alaska: concentrations, pools, origin, and spatial distribution. Global Biogeochem. Cycles 32, 1058–1073. https://doi.org/10.1029/2017GB005840.

Olson, C.L., Jiskra, M., Sonke, J.E., Obrist, D., 2019. Mercury in tundra vegetation of Alaska: spatial and temporal dynamics and stable isotope patterns. Sci. Total Environ. 660, 1502–1512. https://doi.org/10.1016/j.scitotenv.2019.01.058.

Pérez-Rodríguez, M., Biester, H., Aboal, J.R., Toro, M., Martínez-Cortizas, A., 2019. Thalwing of snow and ice caused extraordinary high and fast mercury fluxes to lake sediments in Antarctica. Geochem. Cosmochim. Acta 248, 109–123. https://doi.org/10.1016/j.gca.2019.01.009.

Pérez-Rodríguez, M., Horak-Terra, I., Rodríguez-Lado, I., Aboal, J.R., Martínez-Cortizas, A., 2015. Long-term (ca. 57 ka) controls on mercury accumulation inthe southern hemisphere reconstructed using a peat record from Pinheiro Mire (Minas Gerais, Brazil). Environ. Sci. Technol. 49, 1356–1364. https://doi.org/10.1021/es504826d.

Rasmussen, S.O., Bigler, M., Blockley, S.P., Blunier, T., Buchardt, S.L., Clausen, H.B., Cvijanovic, I., Dahl-Jensen, D., Johnsen, S.J., Fischer, H., Gkinis, V., Guillevic, M., Hoek, W.Z., Lowe, J.J., Pedro, J.B., Popp, T., Seierstad, I.K., Steffensen, J.P., Svensson, A.M., Vallelonga, P., Vinther, B.M., Walker, M.J., Wheatley, J.J., Winstrup, M., 2014. A stratigraphic framework for abrupt climatic changes during the Last Glacial period based on three synchronized Greenland ice-core records: refining and extending the INTIMATE event stratigraphy. Quat. Sci. Rev. 106, 14–28. https://doi.org/10.1016/j.quascirev.2014.09.007.

Reimann, C., Arnoldussen, A., Boyd, R., Finne, T.E., Koller, F., Nordgulen, Ø., Englmaier, P., 2007. Element contents in leaves of four plant species (birch, mountain ash, fern and spruce) along anthropogenic and geogenic concentration gradients. Sci. Total Environ. 377, 416–433. https://doi.org/10.1016/j.scitotenv.2007.02.011.

Reimer, P.J., Austin, W.E.N., Bard, E., Bayliss, A., Blackwell, P.G., Bronk Ramsey, C., Butzin, M., Cheng, H., Edwards, R., Friedrich, M., Grootes, P., Guilderson, T., Hajdas, I., Heaton, T., Hogg, A., Hughen, K., Kromer, B., Manning, S., Muscheler, R., Palmer, J., Pearson, C., van der Plicht, J., Reimer, R., Richards, D., Scott, E., Southon, J., Turney, C., Wacker, L., Adolphi, F., Büntgen, U., Capano, M., Fahrni, S., Fogtmann-Schulz, A., Friedrich, R., Köhler, P., Kudsk, S., Miyake, F., Olsen, J., Reinig, F., Sakamoto, M., Sookdeo, A., Talamo, S., 2020. The IntCal20 northern hemisphere radiocarbon age calibration curve (0–55 cal kBP). Radiocarbon 62 (4), 725–757. https://doi.org/10.1017/RDC.2020.41.

Roman, M., Mirosław-Grabowska, J., Niska, M., 2021. The Eemian lakeland of the central polish plain: environmental changes and palaeogeography. Palaeogeogr. Palaeocl. 561, 110087. https://doi.org/10.1016/j.palaeo.2020.110087.

Roos-Barraclough, F., Martinez-Cortizas, A., García-Rodeja, E., Shotyk, W., 2002. A 14 500 year record of the accumulation of atmospheric mercury in peat: volcanic signals, anthropogenic influences and a correlation to bromine accumulation. Earth Planet Sci. Lett. 202, 435–451. https://doi.org/10.1016/S0012-821X(02)00805-1.

Rychel, J., Karasiewicz, M.T., Krześlak, I., Marks, L., Noryśkiewicz, B., Woronko, B., 2014. Paleogeography of the environment in north-eastern Poland recorded in an Eemian sedimentary basin, based on the example of the Jałówka site. Quat. Int. 328–329, 60–73. https://doi.org/10.1016/j.quaint.2013.09.018.

Skompski, S., 1980. Nowe stanowiska mięczaków z osadów interglacjalnych w zachodniej Polsce. Biul. Inst. Geol. 322, 5–29.

Sobczyk, A., Borówka, R.K., Badura, J., Stachowicz-Rybka, R., Tomkowiak, J., Hrynowiecka, A., Sławińska, J., Tomczak, M., Pitura, M., Lamentowicz, M., Kołaczek, P., Karpińska-Kołaczek, M., Tarnawski, D., Kadej, M., Moska, P., Krąpiec, M., Stachowicz, K., Bieniek, B., Siedlik, K., Bąk, M., Van der Made, J., Kotowski, A., Stefaniak, K., 2020. Geology, stratigraphy and palaeoenvironmental evolution of the Stephanorhinus kirchbergensis-bearing Quaternary palaeolake(s) of Gorzów Wielkopolski (NW Poland, central Europe). J. Quat. Sci. 35 (4), 539–558. https://doi.org/10.1002/jqs.3198.

Sokołowski, R.J., Hrynowiecka, A., Fedorowicz, S., Jurys, L., 2015. Stratigraphy, sedimentation, paleoenvironments and paleogeographical expression of the Pleistocene sediments at the site of Łęczyce near Lębork. In: INQUA Peribaltic 2015 Working Group Meeting & International Field Symposium, Quaternary Geology and Modern Questions, 2–8. November 2015, Utrecht-Assen, Netherlands, pp. 45–46.

Stefaniak, K., Stachowicz-Rybka, R., Borówka, R.K., Hrynowiecka, A., Sobczyk, A., Moskal-del Hoyo, M., Kotowski, A., Nowakowski, D., Krajcarz, M.T., Billia, E.M.E., Persico, D., Burkanova, E.M., Leschinskiy, S.V., van Asperen, E., Ratajczak, U., Shpansky, A.V., Lempart, M., Wach, B., Niska, M., van der Made, J., Stachowicz, K., Lenarczyk, J., Piątek, J., Kovalchuk, O., 2020. Browsers, grazers or mix-feeders? Study of the diet of extinct Pleistocene Eurasian forest rhinoceros Stephanorhinus kirchbergensis (Jäger, 1839) and woolly rhinoceros Coelodonta antiquitatis (Blumenbach, 1799). Quat. Int. 501, 193–207. https://doi.org/10.1016/j.quaint.2017.10.039.

Tabolt, J., Moore, T.R., Wang, M., Dallaire, C.O., Riley, J.L., 2017. Distribution of lead and mercury in Ontario peatlands. Environ. Pollut. 231, 890–898. https://doi.org/10.1016/j.envpol.2017.08.095.

Talbot, M.R., Laerdal, T., 2000. The Late Pleistocene e Holocene paleolimnology of Lake Victoria, East Africa, based upon elemental and isotopic analyses of sedimentary organic matter. J. Paleolimnol. 23, 141–164. https://doi.org/10.1023/A:1008029400463.

Urbański, K., Winter, H., 2005. The Eemian Interglacial in the section Radówek (Łagów lakeland, western Poland) and its implication for till lithostratigraphy. Prz.Geol. 53, 418–424 [In Polish with English summary].

van der Hammen, T., 1995. The Dinkel valley revisited: Pleniglacial stratigraphy of the eastern Netherland and global climatic change. Mededelingen Rijks Geologische Dienst 52, 343–355.

Wachecka-Kotkowska, L., Krzyszkowski, D., Malkiewicz, M., Mirosław-Grabowska, J., Niska, M., Krzymińska, J., Myśkow, E., Raczyk, J., Wieczorek, D., Stoiński, A., Rzodkiewicz, M., 2018. An attempt to reconstruct the late Saalian to Plenivistulian (MIS6-MIS3) natural lake environment from the "Parchliny 2014" section, central Poland. Quat. Int. 467 (A), 5–25. https://doi.org/10.1016/j.quaint.2016.06.013.

Winter, H., Dobracka, E., Ciszek, D., 2008. Multiproxy studies of Eemian and early Vistulian sediments at Rzecino site (Łobez Upland, western Pomerania lakeland). B. Państ. Inst. Geol. 42, 93–110.

Woronko, B., Rychel, J., Karasiewicz, T.M., Kupryjanowicz, M., Adamczyk, A., Fiłoc, M., Marks, L., Krzywicki, T., Pochocka-Szwarc, K., 2018. Post-Saalian transformation of dry valleys in eastern Europe: an example from NE Poland. Quat. Int. 467, 161–177. https://doi.org/10.1016/j.quaint.2016.09.054.

Zaccone, C., Santoro, A., Cocozza, C., Terzano, R., Shotyk, W., Miano, T.M., 2009. Comparison of Hg concentrations in ombrotrophic pest and corresponding humic acids, and implications for the use of bogs as archives of atmospheric Hg deposition. Geoderma 148, 399–404. https://doi.org/10.1016/j.geoderma.2008.11.017.

Żarczyński, M., Wacnik, A., Tylmann, W., 2019. Tracing lake mixing and oxygenation regime using the Fe/Mn ratio in varved sediments: 2000 year record of human-induced changes from Lake Żabińskie (NE Poland). Sci. Total Environ. 657, 585–596. https://doi.org/10.1016/j.scitotenv.2018.12.078.

Żarski, M., Winter, H., Kucharska, M., 2018. Palaeoenvironmental and climate changes recorded in the lacustrine sediments of the Eemian Interglacial (MIS 5e) in the Radom Plain (Central Poland). Quat. Int. 467, 147–160. https://doi.org/10.1016/j.quaint.2016.12.001.